THE HIGH REDSHIFT UNIVERSE

Hubble Ultra Deep Field
Hubble Space Telescope • Advanced Camera for Surveys

NASA, ESA, S. Beckwith (STScI) and the HUDF Team

STScI-PRC04-07a

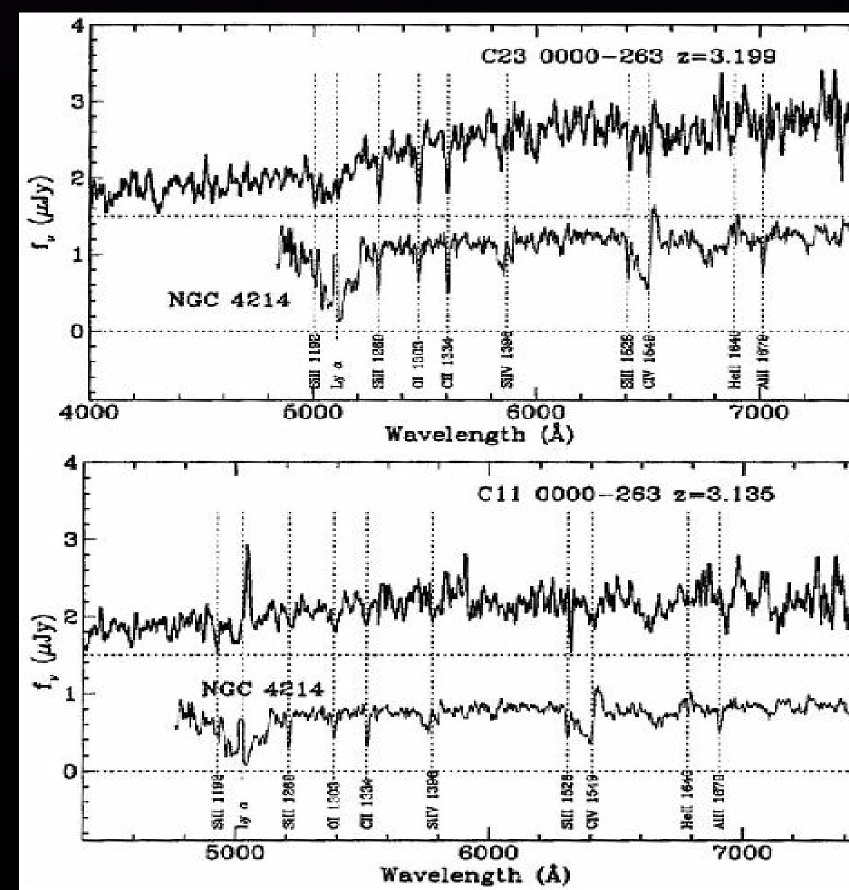

The first phase change of hydrogen in the universe was **recombination,** which occurred at a redshift $z = 1089$ (379,000 years after the Big Bang), due to the cooling of the universe to the point where the rate of recombination of electrons and protons to form neutral hydrogen was higher than the re-ionization rate.

The second phase change occurred once objects started to condense in the early universe that were energetic enough to ionize neutral hydrogen. As these objects formed and radiated energy, the universe reverted from being neutral, to once again being an ionized plasma. This occurred between 150 million and one billion years after the Big Bang (at a redshift $6 < z < 20$). This is commonly referred to as the epoch of **re-ionization.**

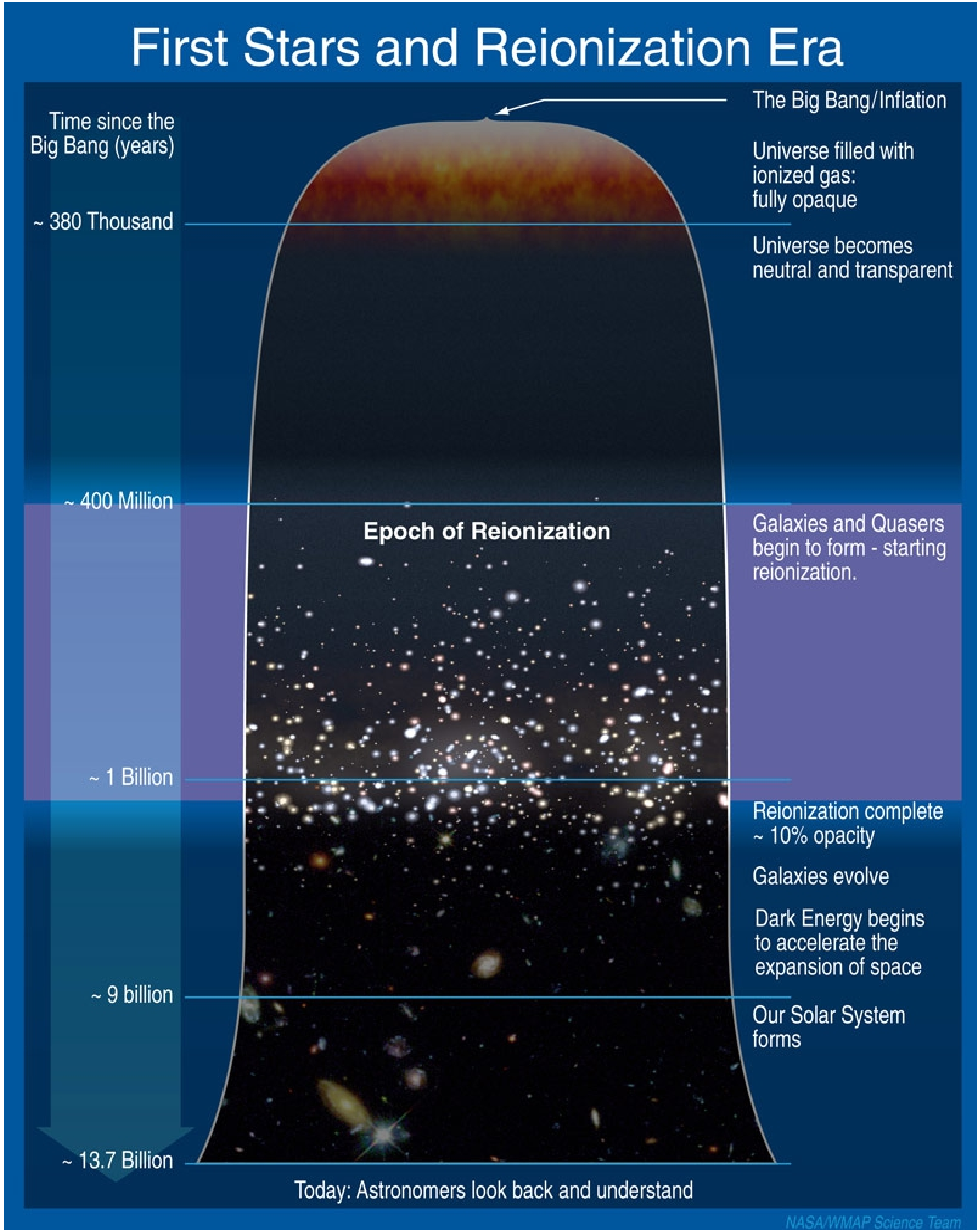
First Stars and Reionization Era
Time since the Big Bang (years)
~ 380 Thousand
~ 400 Million
~ 1 Billion
~ 9 billion
~ 13.7 Billion
The Big Bang/Inflation
Universe filled with ionized gas: fully opaque
Universe becomes neutral and transparent
Epoch of Reionization
Galaxies and Quasars begin to form - starting reionization.
Reionization complete ~ 10% opacity
Galaxies evolve
Dark Energy begins to accelerate the expansion of space
Our Solar System forms
Today: Astronomers look back and understand
NASA/WMAP Science Team

Scenario

1. At the Recombination Epoch at z ~ 1100 protons and electrons recombine and the Universe gets transparent for optical light
2. The period from recombination to z ~ 20 -30 presents a Universe with no (easily) visible structures.
3. At redshift 20 – 30 the first cloud collapse in Dark Matter „Minihalos" leads to the formation of the first stars.

   These stars have larger masses and are refered to as Pop III stars.
4. At redshifts ~ 15 larger Dark Matter haloes form in which stars form from already metal enriched gas (Pop II stars).
5. The UV radiation from massive stars and star bursts as well as from acctreting massive black holes blows Stroemgren spheres into the gas in the Universe.
6. The Stroemgren spheres start to overlap, the intergalactic medium gets more and more ionized and the Universe becomes transparent to Lα-radiation.

Observations of Extinction of UV-Flux From Distant Objects

- The spectrum of QSO get absorbed at the short wavelength side of the Ly-α Line due to resonant scattering at HI atoms -- „Gunn-Peterson Effekt“ (1965). At lower redshift we observe distinct absorption droughs (Ly-α absorbing clouds) which become more and more frequent at higher redshift and merge into a dense absorbing curtain at redshift ~ 6.

Absorption is given by:

$$I_{abs} = I_{em}(1 - e^{-\tau_{HI}}) \qquad \tau_{HI}(z) \sim 6.5 \cdot 10^5 \frac{n_{HI}}{n_H} \left(\frac{1+z}{10} \right)^{1.5}$$

Intergalactic Neutral Hydrogen Absorption

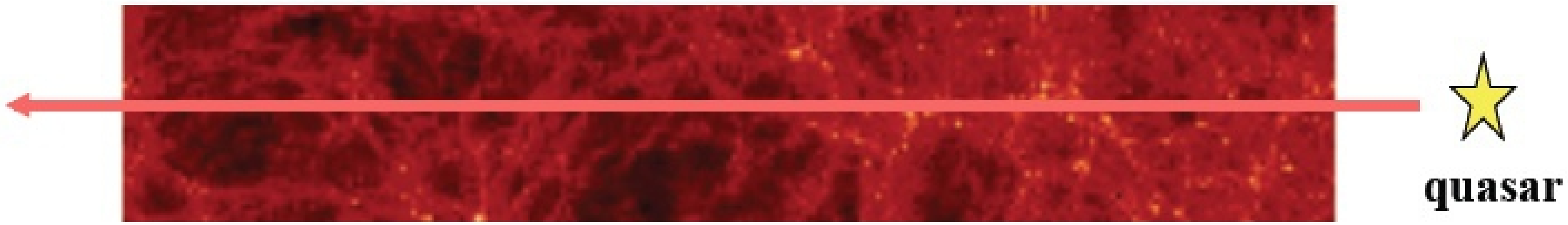

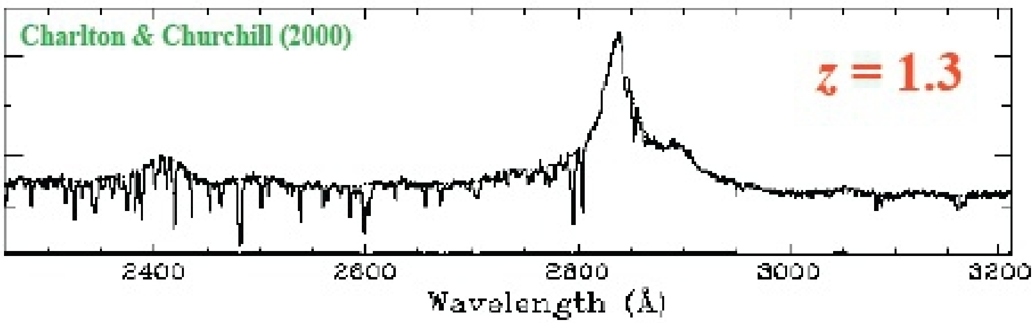

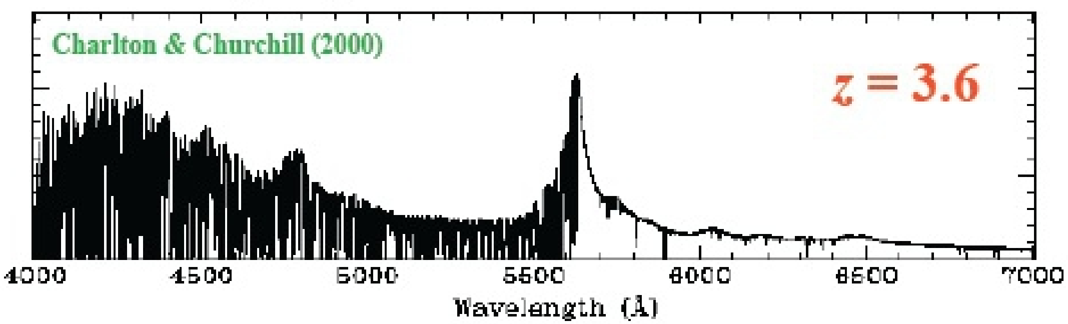

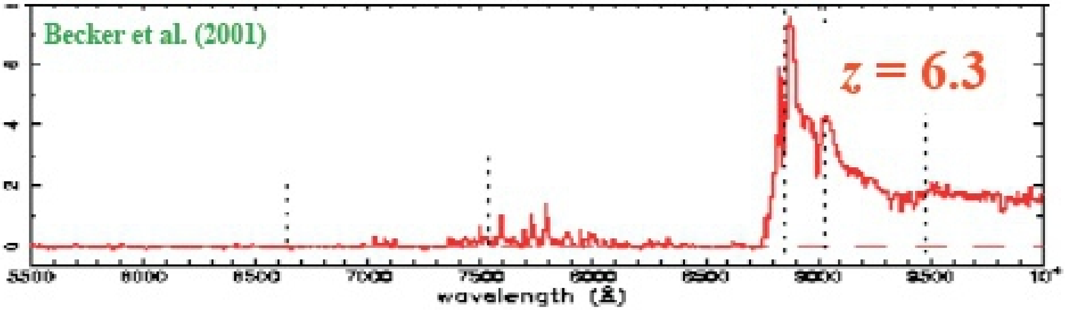

Ly-α Absorption in the Spectra of SDSS QSO

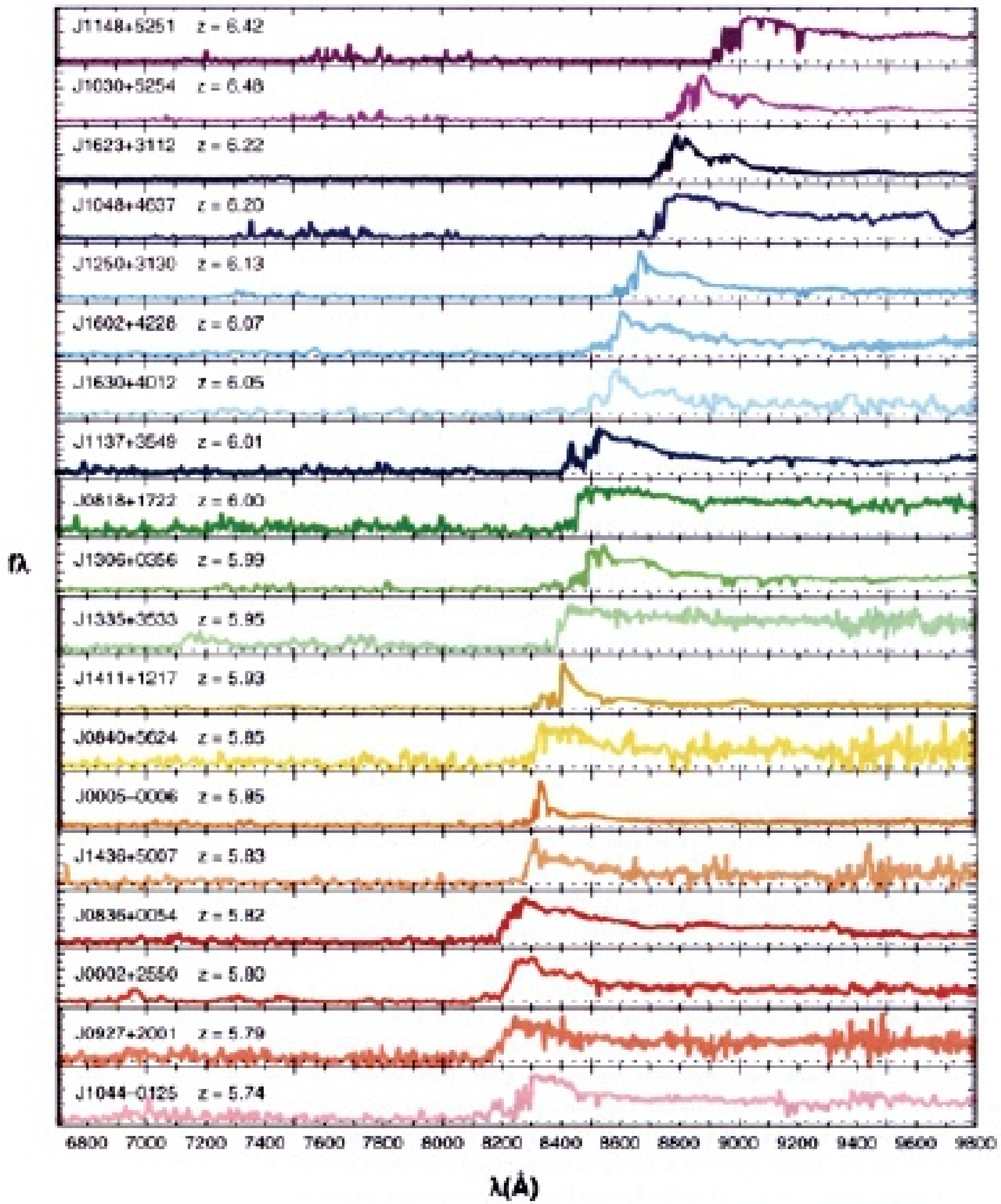

19 spectra of QSO in the redshift range 5.74 to 6.42 frm the Sloan Digital Sky Survey (SDSS) from Fan et al. 2006. The highest redshift QSO show nearly complete Gunn-Peterson troughs. The data illustrate the increasing opaquness of the Universe to Ly-α radiation with increasing redshift.

Ly-a Transparency of the Universe

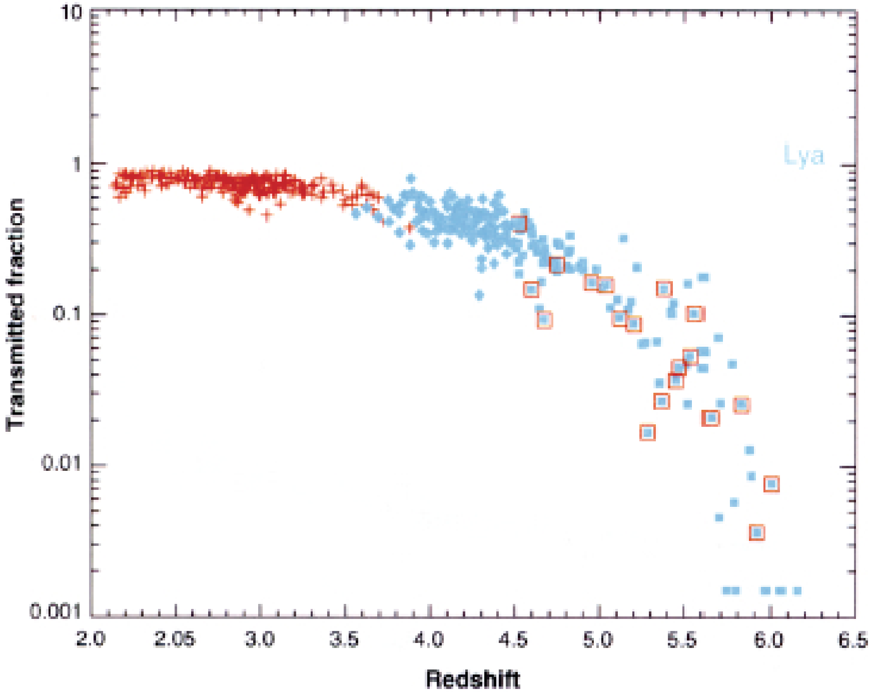

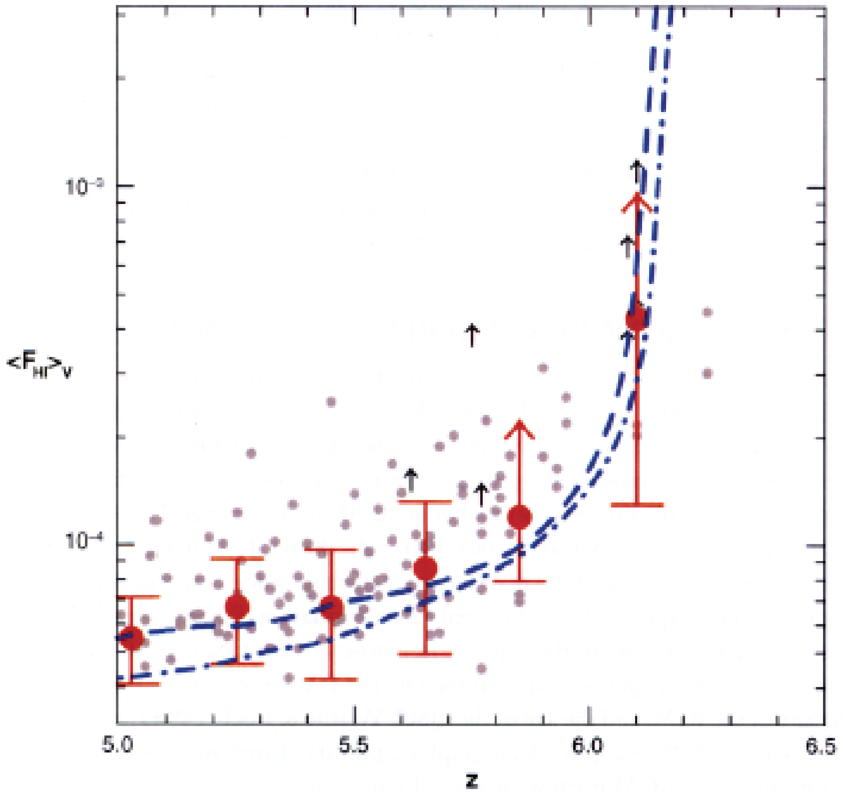

Transparency and hydrogen ionization fraction of the Universe in the redshift range probe by SDSS QSO (Fan et al. 2006). The Reionization of the Universe is nearly completed at redshifts z = 5-6.

Future Possibility to Study the HI Universe at the Reionization Epoch in the 21cm line (e.g. with SKA)

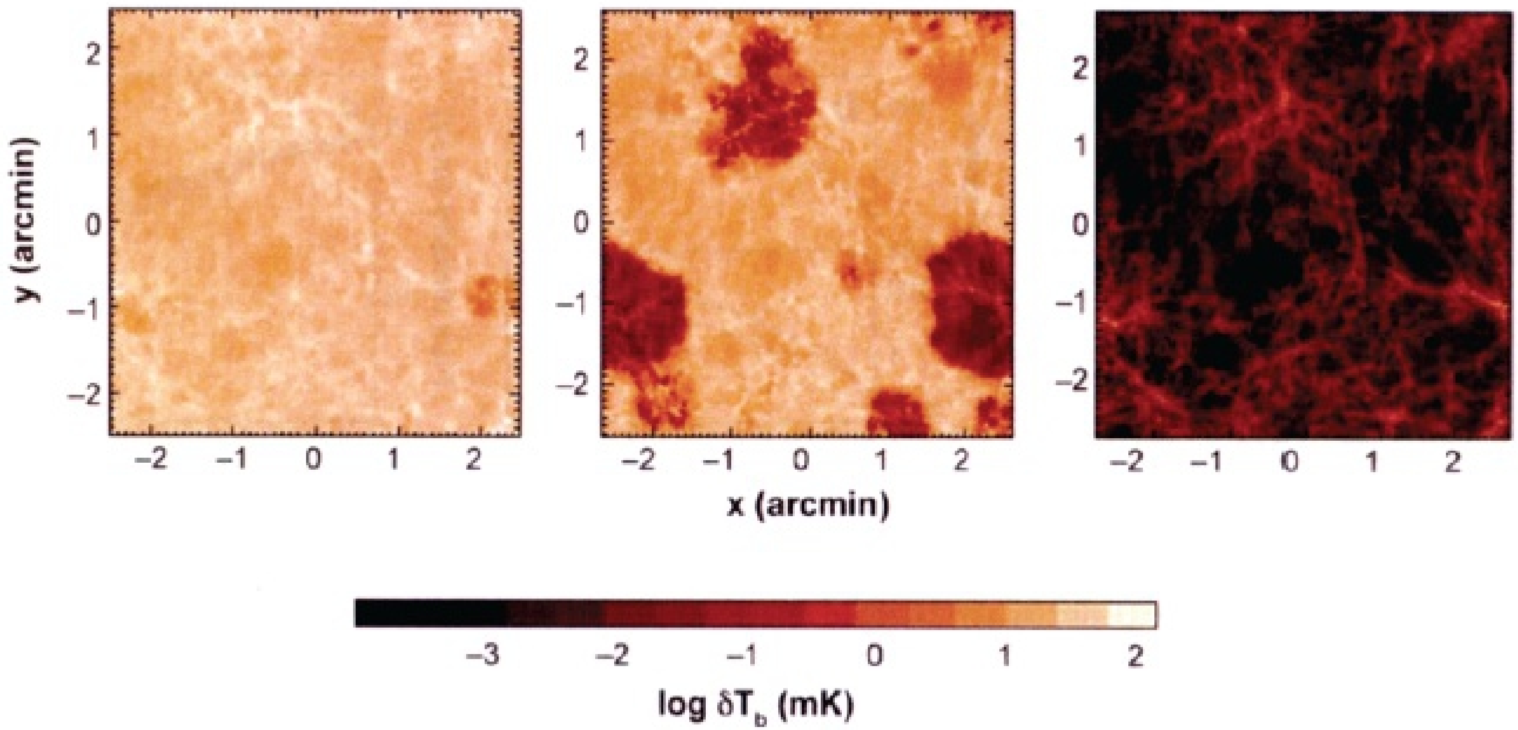

Simulation of the 21cm brightness temperature distribution in the sky during the epoch of reionization at redshifts: 12, 9, 7 [by Furlanetto et al. 2004]. The planned Square Kilometer Area radio interferometer (SKA) can possibly see this radiation. Much effort may be needed to clearly detect this radiation in the presence of various foregrounds.

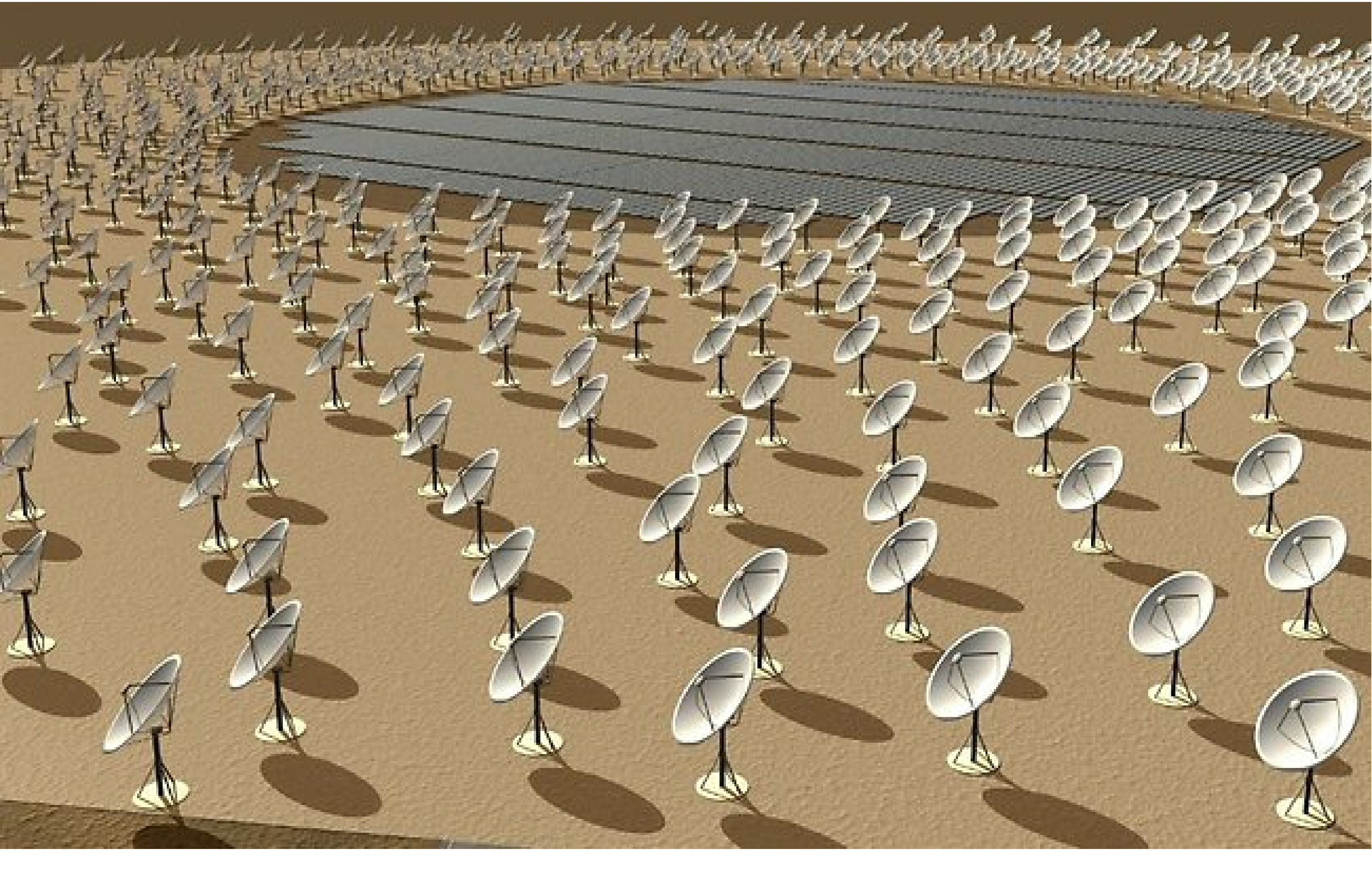

The Formation of the First Stars

- The seeds that eventually lead to stars and galaxies are the fluctuations imprinted in the CMB.
- The dynamics of both the dark matter (DM) and the baryons have to be considered.
- Dark matter halos are the sites of star formation.
- The baryon collapse inside halos is governed by the thermal-chemical properties of the gas, including shocks.
- An analog with local star formation: baryon core - DM halo, with molecule formation playing a key role.
- This model of star formation is developed by generalizing the ΛCDM simulations to include the necessary atomic and molecular physics required to treat the formation of molecules and their thermal consequences.

Formation of H_2

Starting from warm (< 3000 K) and moderately dense (275 cm^{-3}) atomic hydrogen and helium gas *without dust grains*, molecules can form by weak radiative processes

The first molecule produced at the onset of cosmic recombination was the molecular ion HeH^+, soon followed by H_2^+

$$He^+ + H \rightarrow HeH^+ + h\nu \qquad k \cong 2\text{x}10^{-16}\ \text{cm}^3\text{s}^{-1} \quad \text{(at 3000 K)}$$

$$He + H^+ \rightarrow HeH^+ + h\nu \qquad k \cong 4\text{x}10^{-17}\ \text{cm}^3\text{s}^{-1}$$

$$H^+ + H \rightarrow H_2^+ \qquad k \cong 2\text{x}10^{-16}\ \text{cm}^3\text{s}^{-1}$$

These ions are destroyed by dissociative recombination, photodissociation and by reaction with H to form H_2^+:

Molecule Production in the Recombination Era

Lepp, Stancil & Dalgarno (2002)

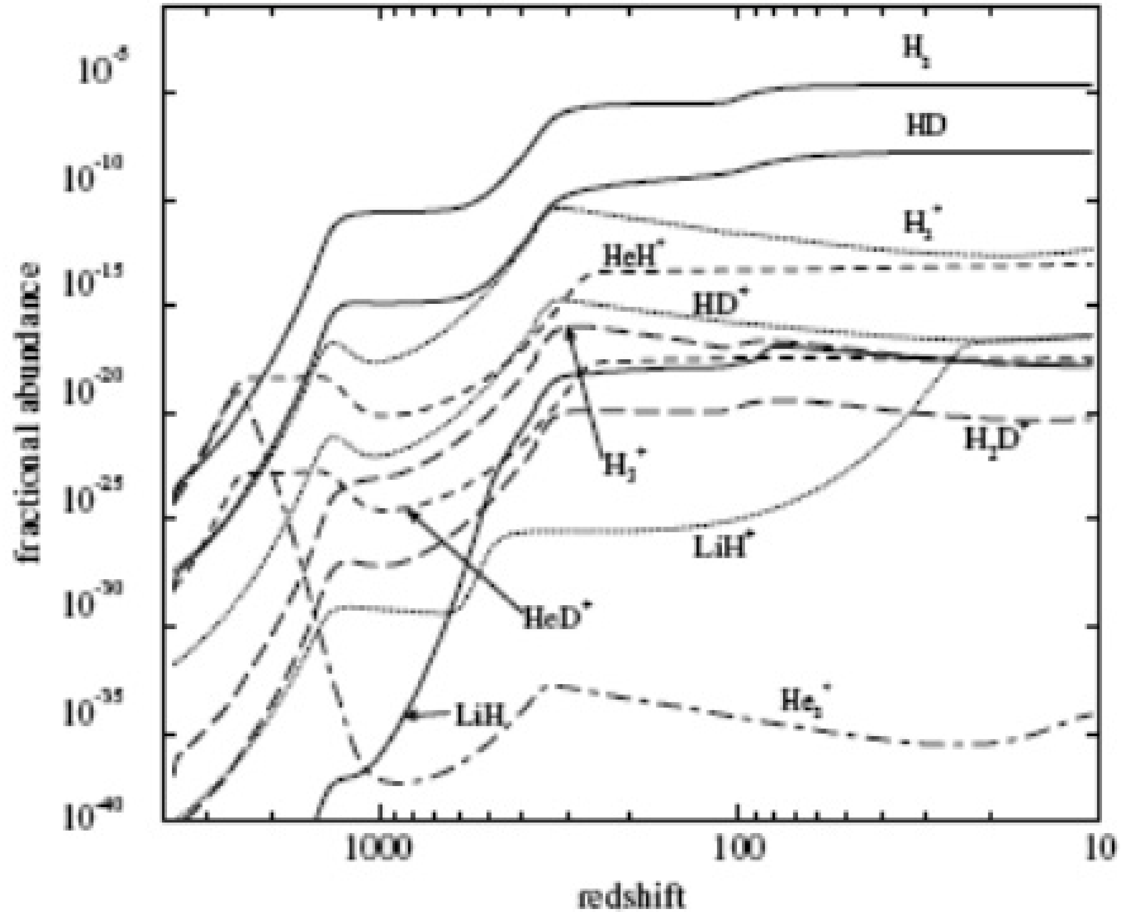

The most abundant species in decreasing order are:

$H : He : H+ : D : H_2 : HD =$

$1 : 0.08 : 4 \times 10^{-4} : 4 \times 10^{-5} : 10^{-5} : 2 \times 10^{-8}$

High Resolution Simulation of One Halo

With Loads of Physics (Yoshida et al. 2006)

- Simulation at z = 15 in a 0.3 Mpc cube with 60 $M_{\oplus}$ resolution
- focus on a single DM halo of 600,000 M_{sun}
- central part of top right panel has 300 M_{sun} and diameter ~ 1 pc and is collapsing
- collapsing core does not fragment nor form a disk (low ang. mom.)
- estimated stellar mass ~ 300 M_{sun}

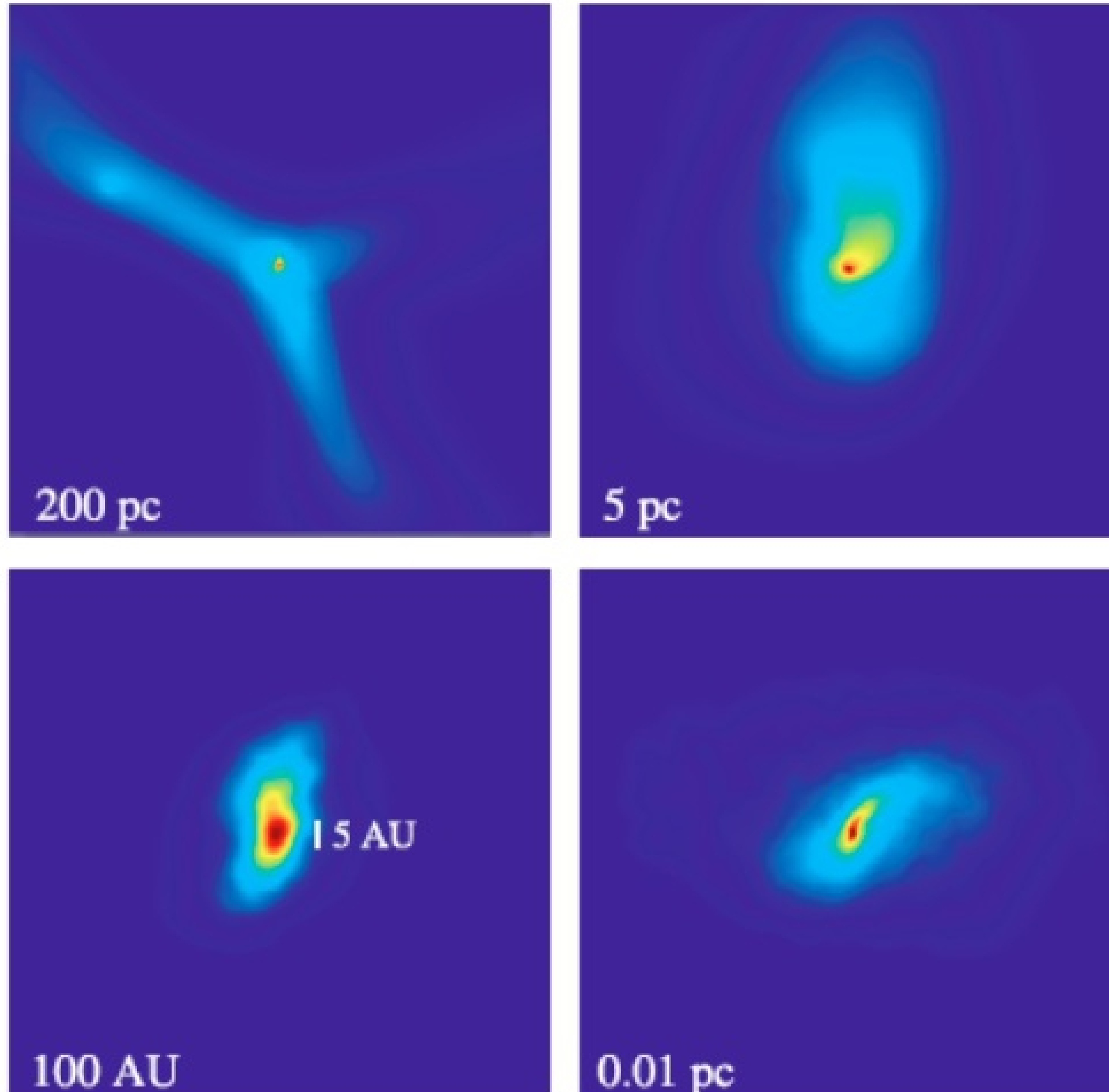

Simulation Including Ionizing Radiation:
HII Region of the First Star z = 26

Yoshida et al. ApJ 663 687 2007

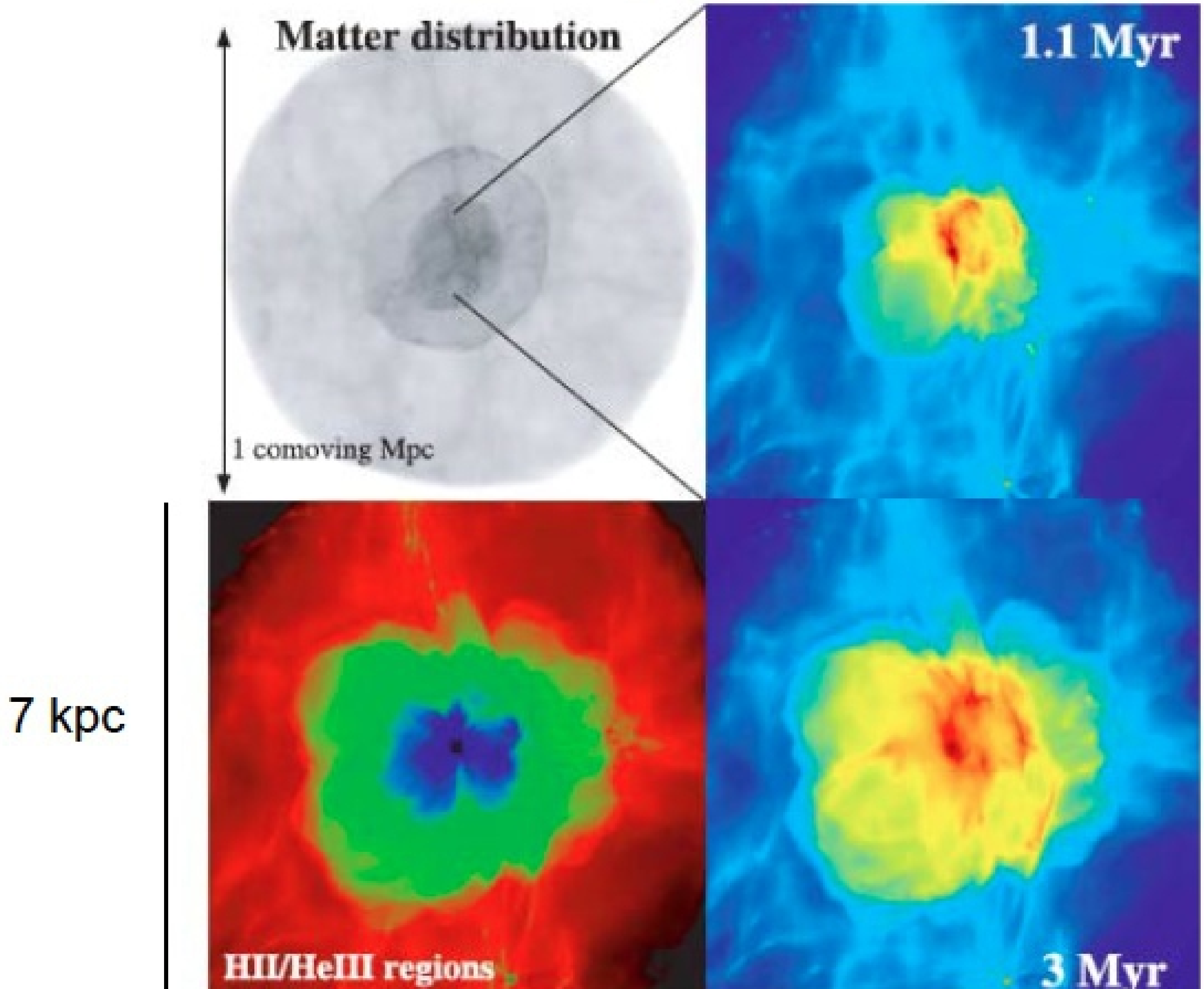

Protostars from Dark Matter Simulations

Yoshida et al. 2007

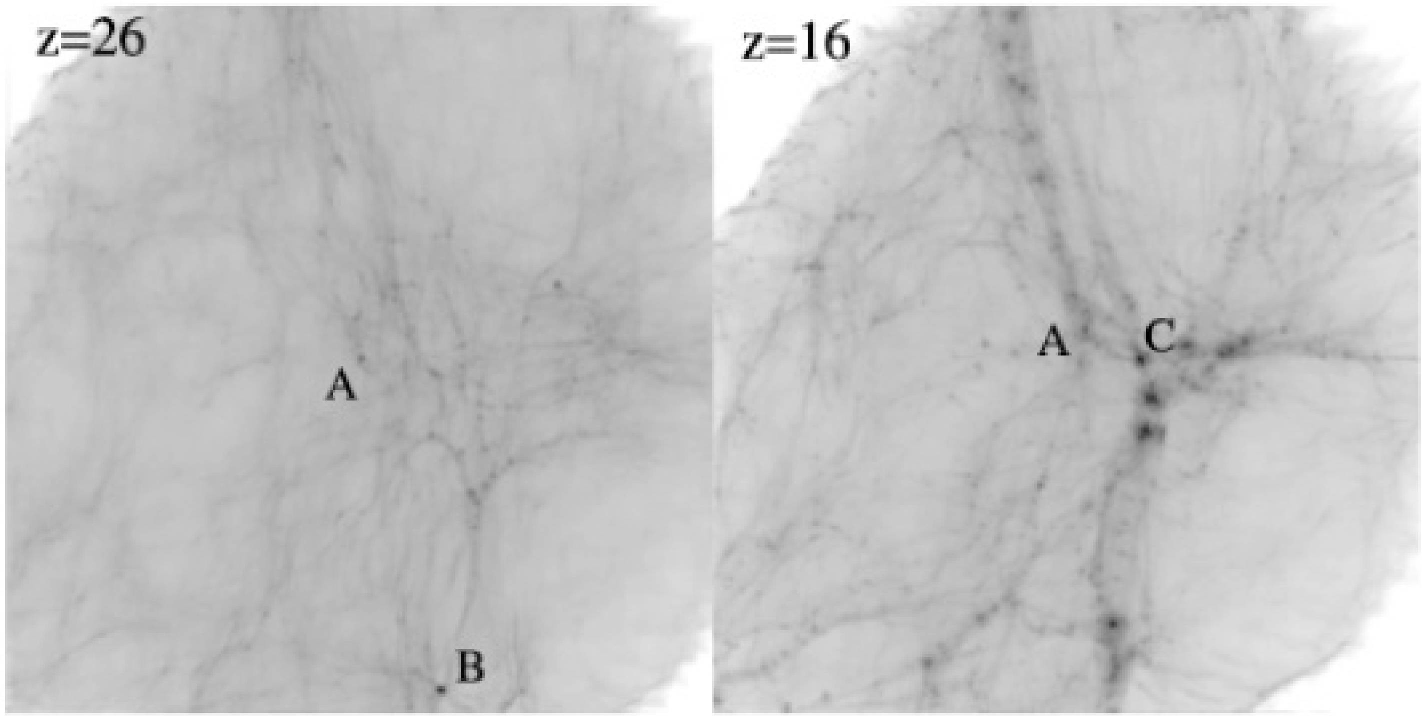

Change in DM evolution over 100 Myr, including effects of the ionizing radiation from the first star formed in halo A. A second generation star forms in nearby halo C under changed physical conditions. **More generally, the time from the first star to complete reionization is several hundred Myr.**

Summary

- The simulation of early star formation from baryonic cores inside dark matter halos involves the complicated atomic and molecular and radiation physics of a cooling and chemically active collapsing gas cloud.
- The results are incomplete, in part because present simulations can only treat small regions of the pre-IGM.
- Although the results are not yet definitive, they are convincing in indicating that stars (and presumably galaxies) can form at moderately-high redshifts.

REIONIZATION OF THE UNIVERSE ON LARGE SCALES

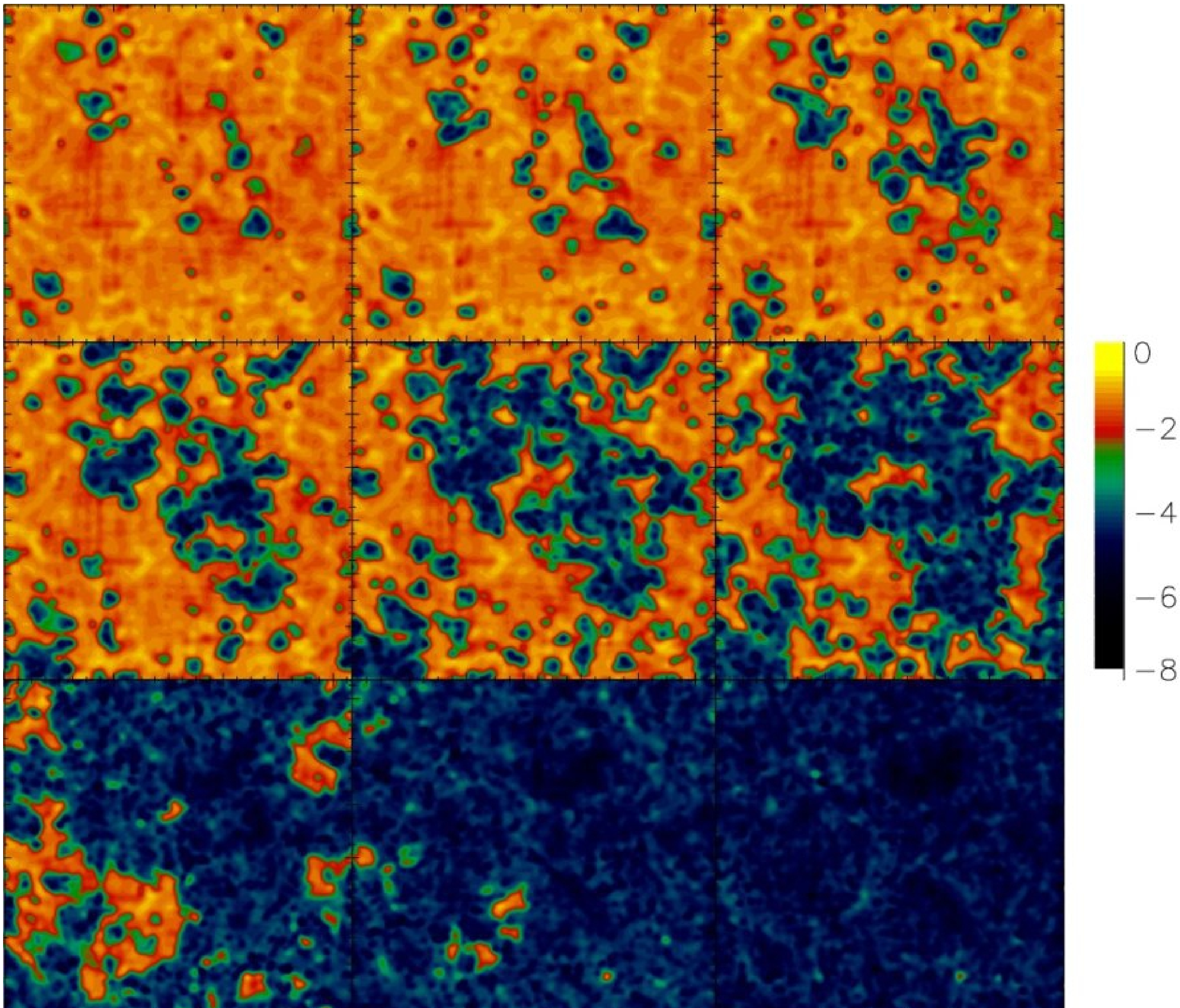

The Hunt for the Highest Redshift Galaxies

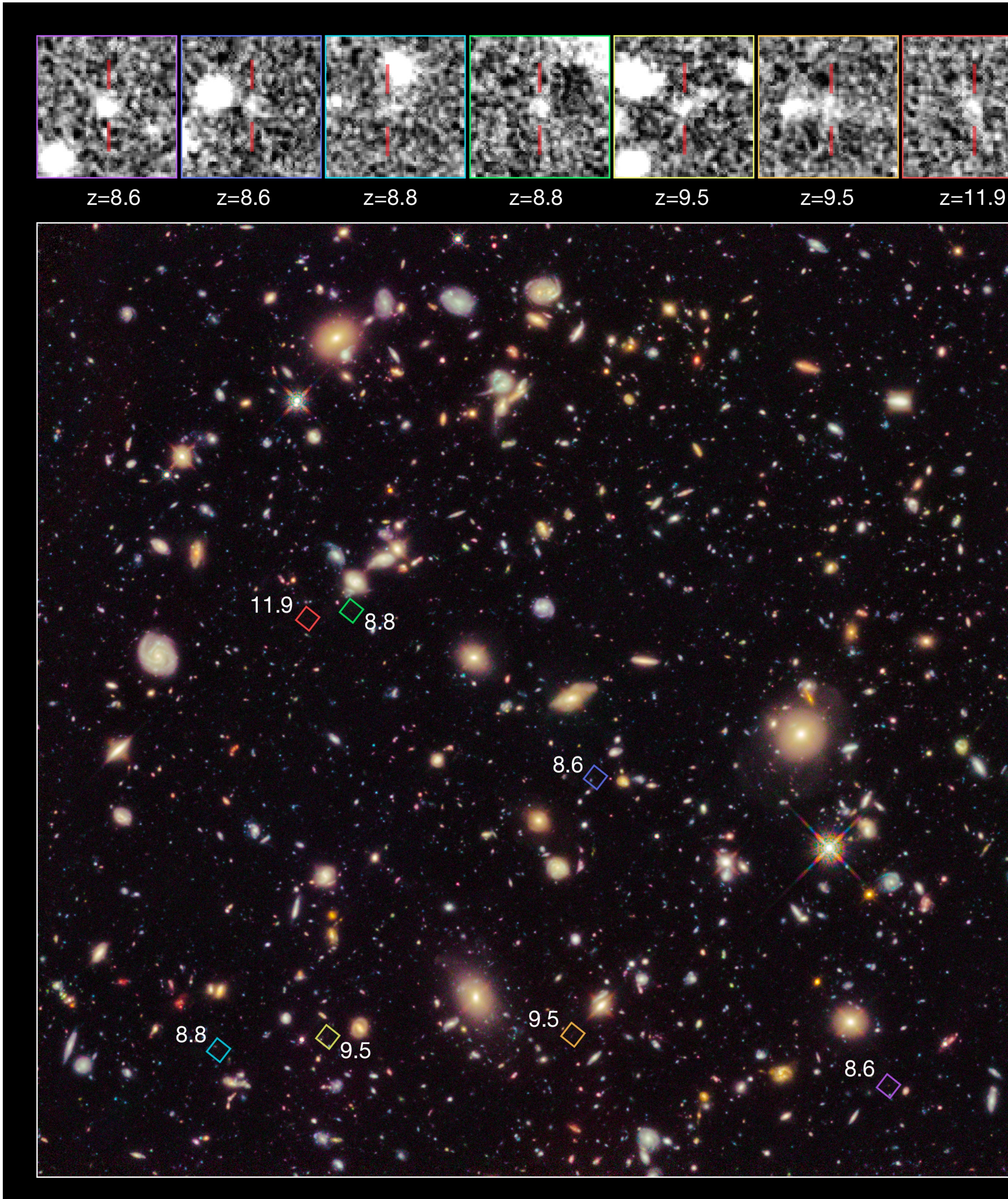

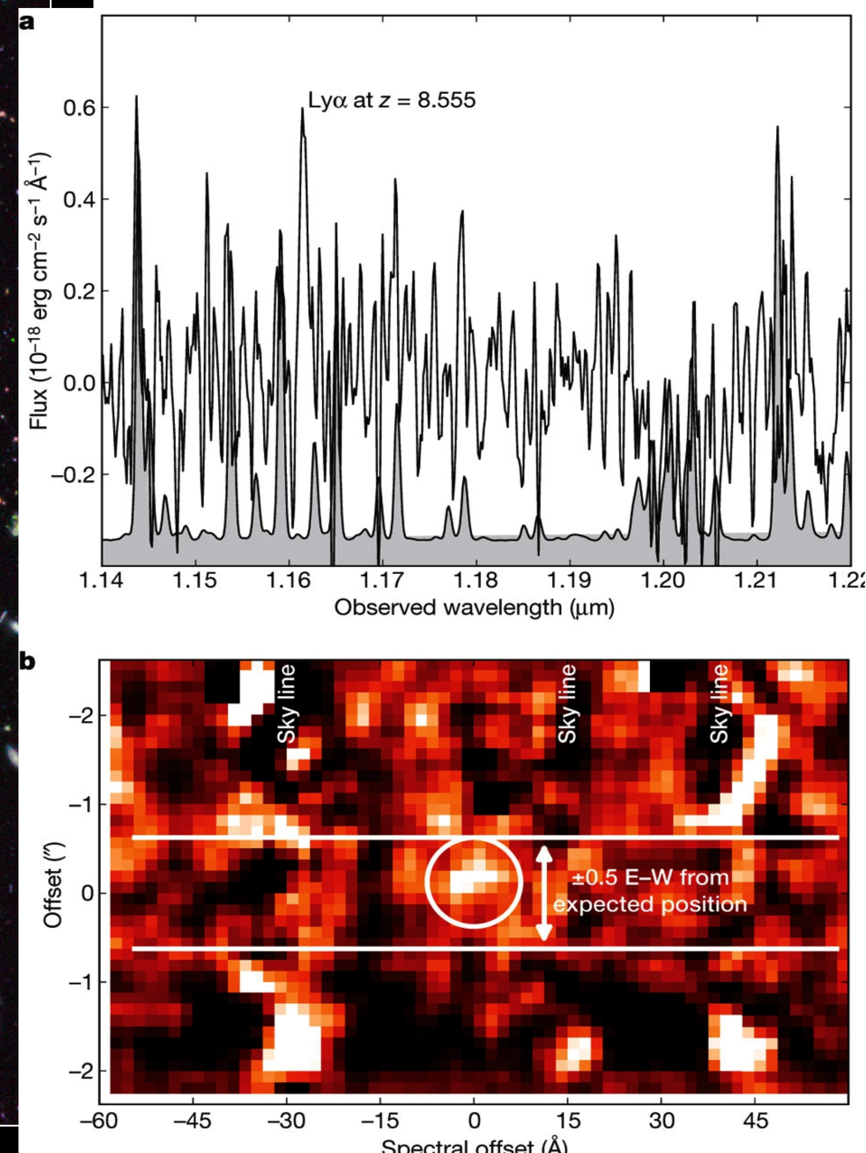

GALAXY EVOLUTION ACROSS COSMIC TIME

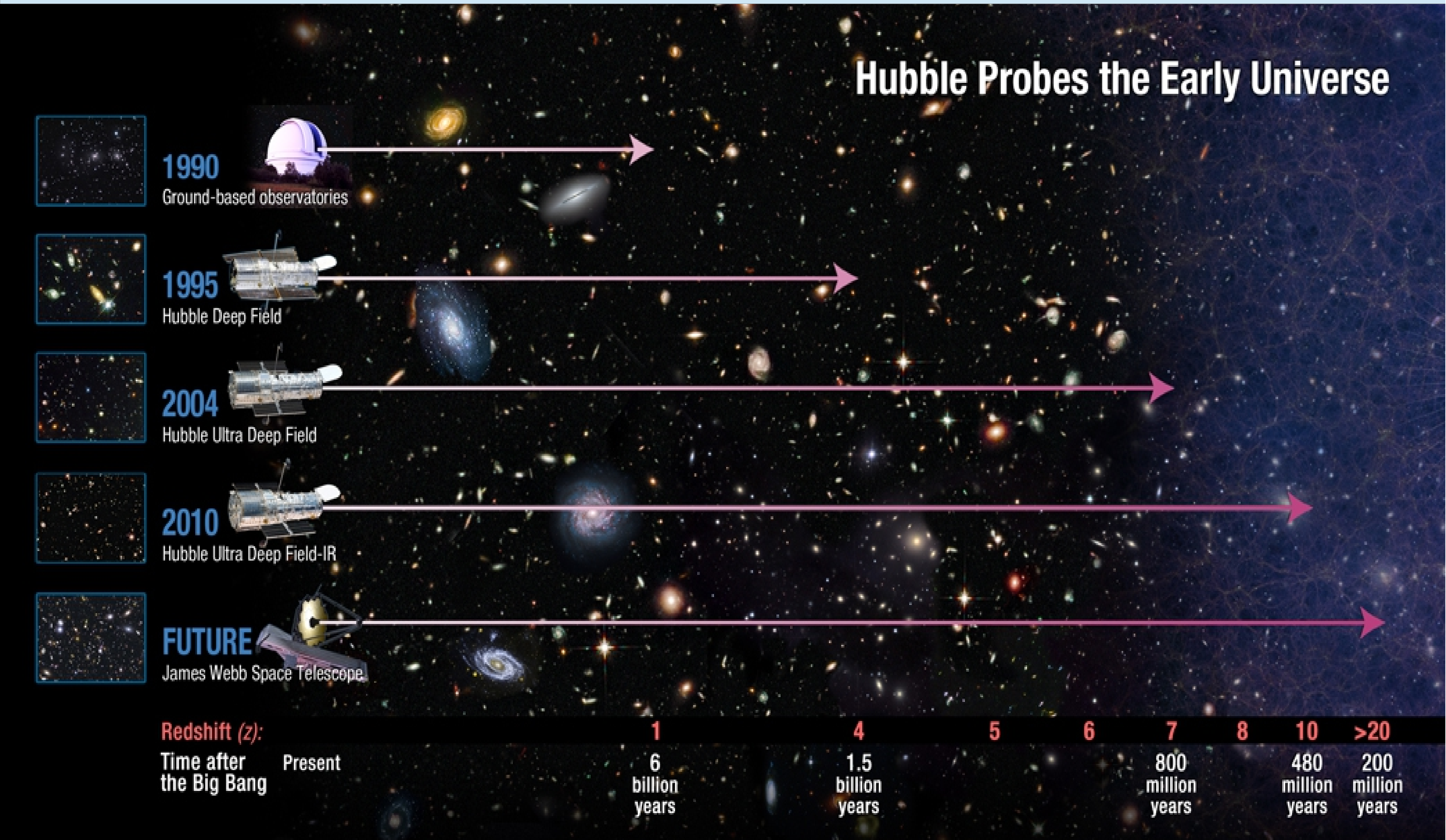

Finding high redshift galaxies:

1) The Lyman Break Technique

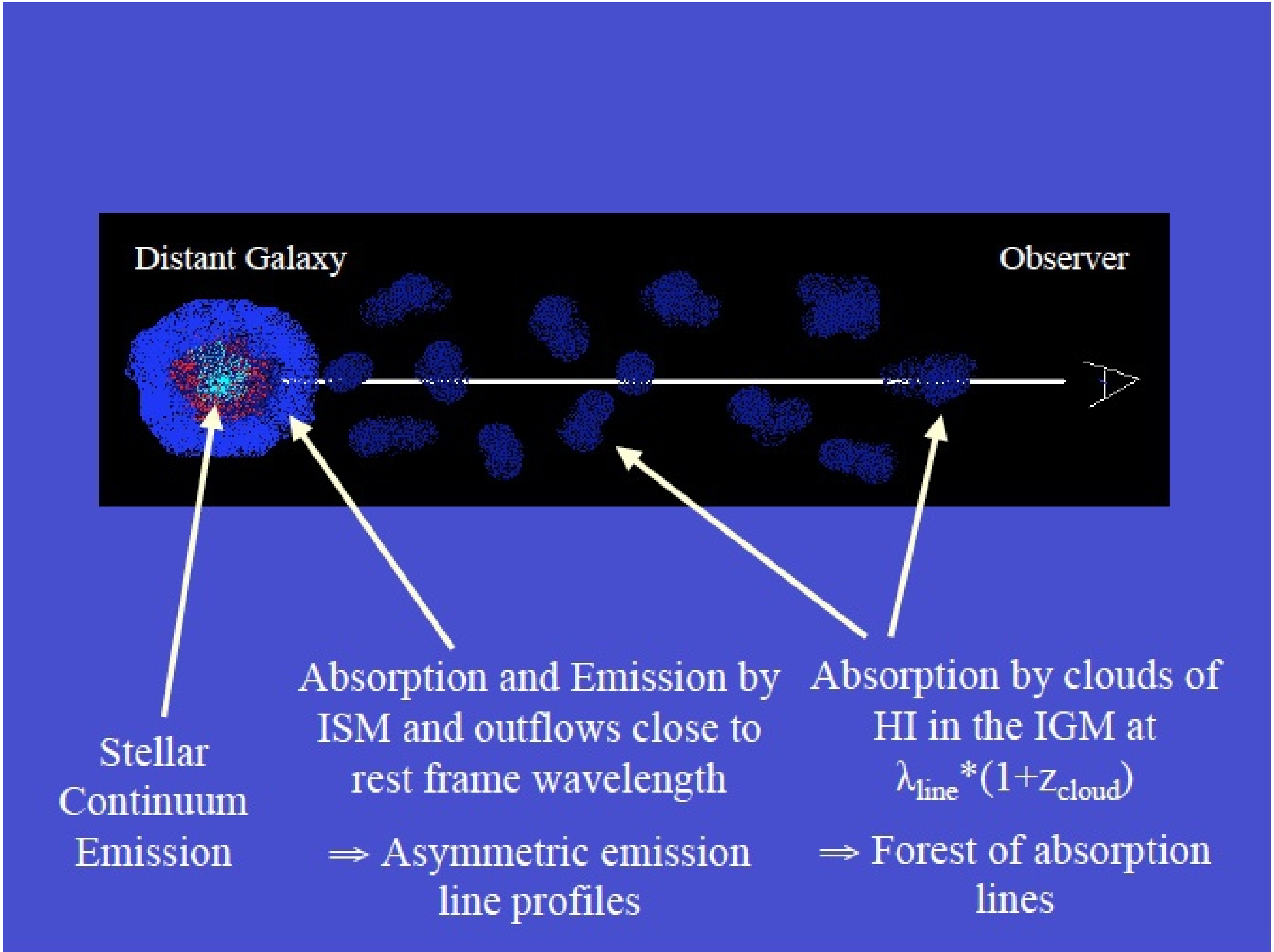

Intergalactic absorption provides a huge marker at high z

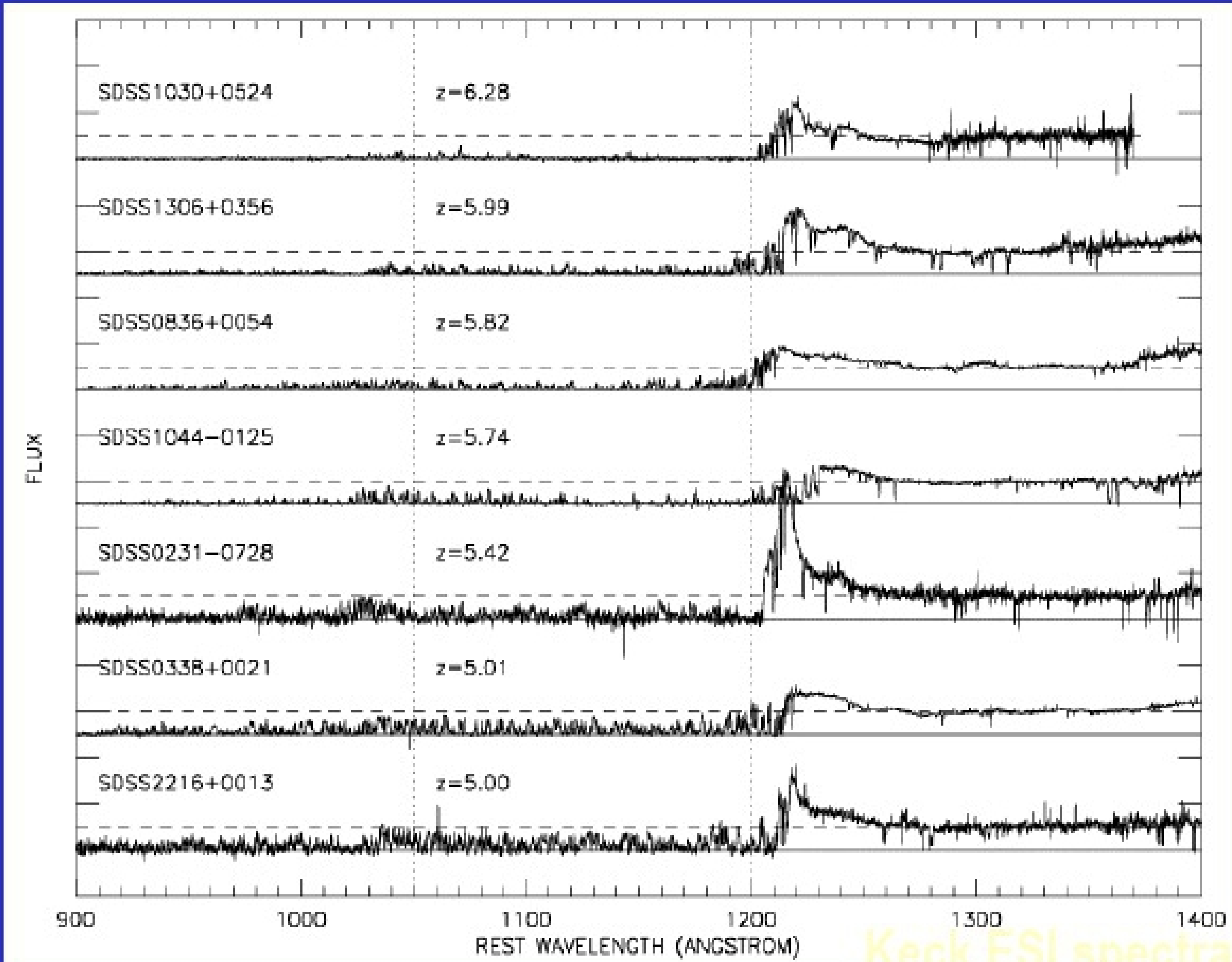

Lyman break galaxies

- Galaxy is visible in the two longer wavelength filters.
- Due to young stellar population, galaxy appears blue in these two filters.
- Expect galaxy to be brighter at shorter wavelengths, but it disappears or “drops out” due to absorption shortward of Ly α.
- Called Lyman break or drop out galaxies.
- Very effective technique to find large numbers of high z galaxies.
- Select z of interest by choosing filter bands.
- First done with U-band, so Lyman break often refers to galaxies found at $z \sim 3$.

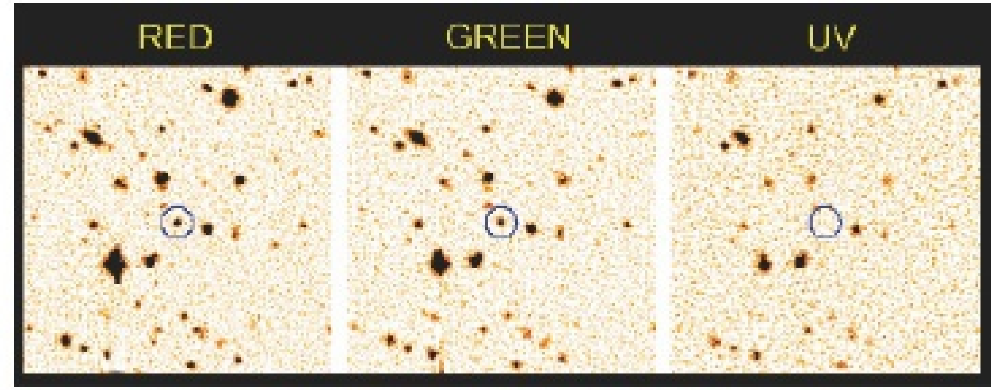

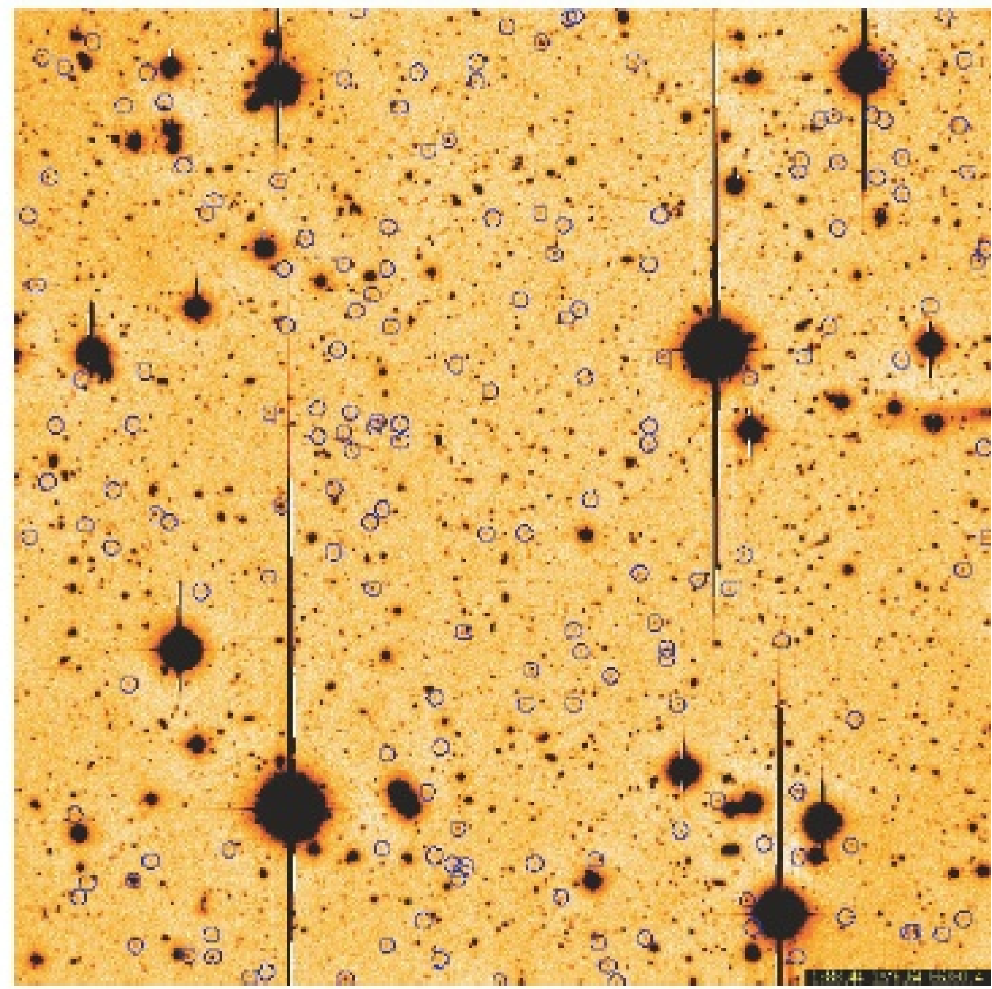

Lyman break galaxies

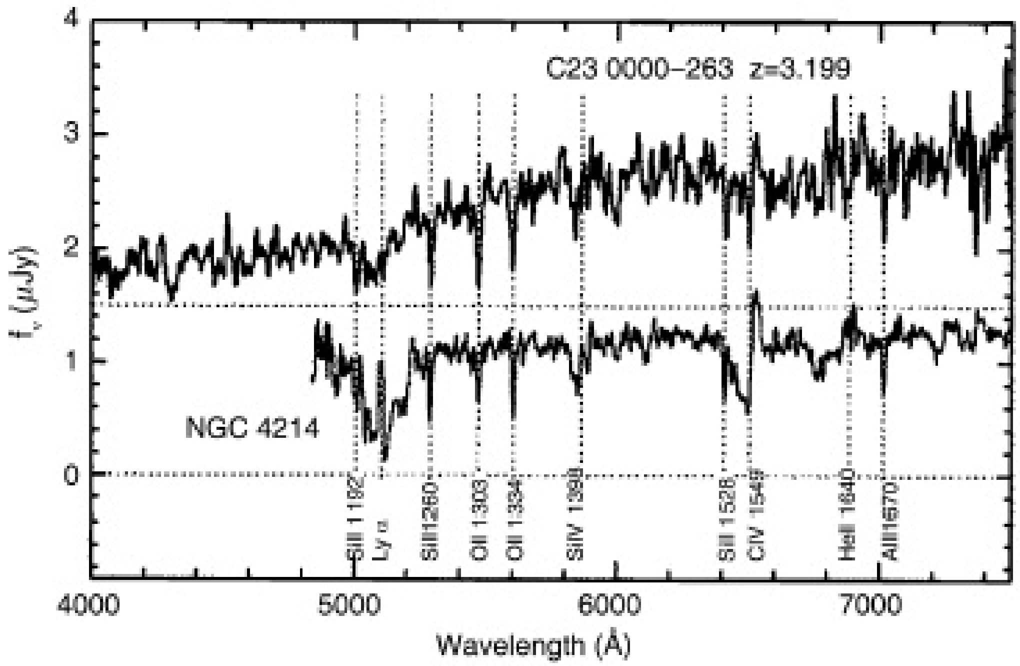

- Redshifts can be confirmed spectroscopically.
- Spectrum also reveals galaxy type.
- Tend to find star forming galaxies.
- Spectra are (typically) very similar to nearby star forming galaxies.
- Many of the galaxies lack a Ly α emission line.

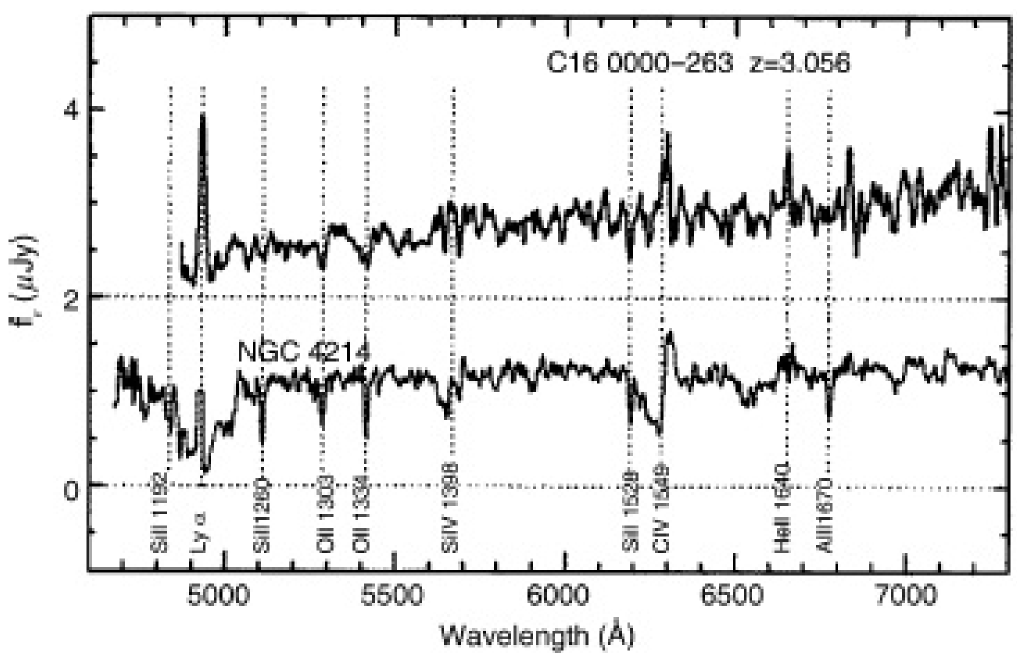

2) Photometric redshifts

- Galaxies tend to have spectral features at the Lyman edge (~1000 Å) and at the Balmer edge (~4000 Å).
- Using photometry in multiple bands, preferably covering the optical and NIR, one can use these features to determine the galaxy redshift.
- The overall shape is determined by the galaxy type, so one fits for redshift and galaxy type simultaneously.

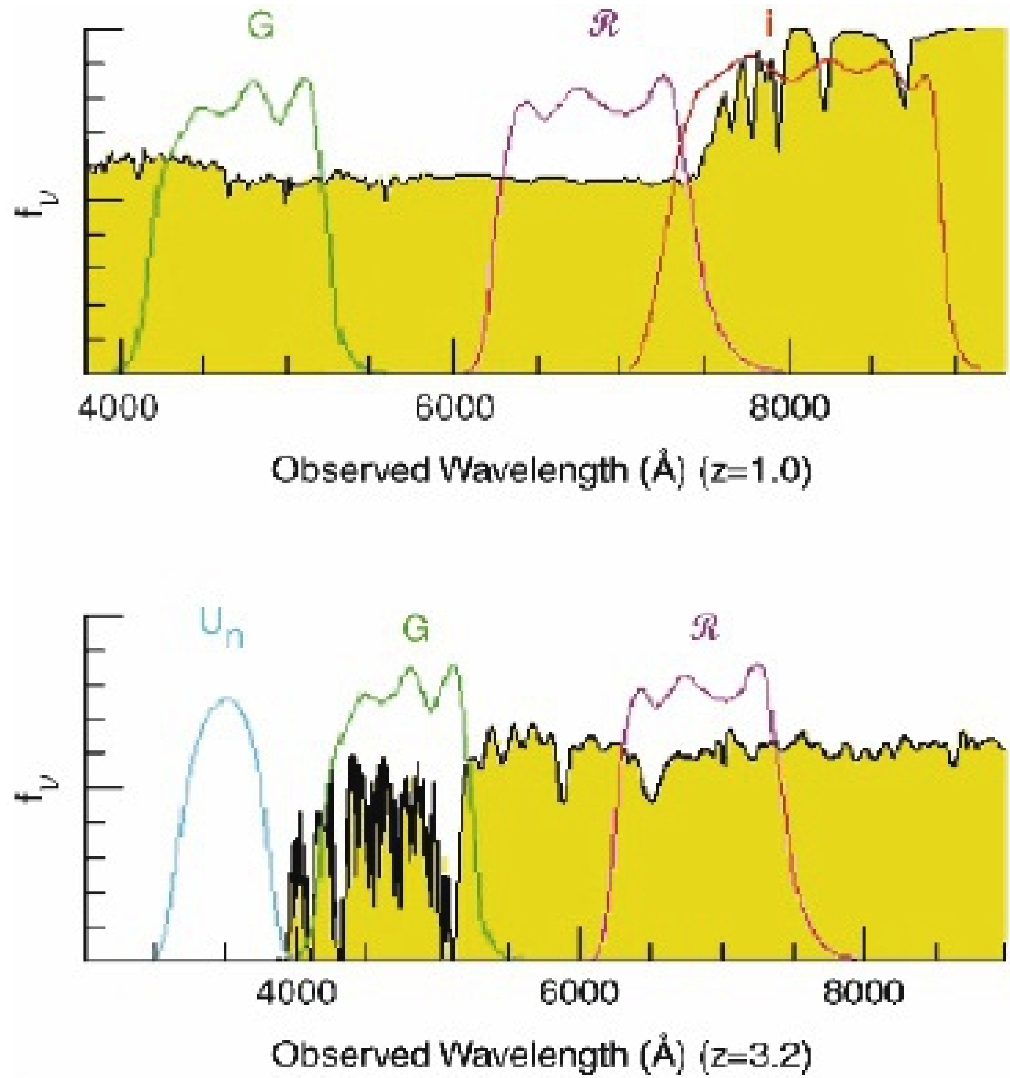

Catalog Overview

The current catalog release, v4.1 is a Ks-selected catalog of the COSMOS field based on the imaging from the DR1 UltraVISTA release. The catalog covers a total area of 1.62 deg^2, and has photometry in 30 bands including the GALEX, Subaru, CFHT, UltraVISTA, and Spitzer imaging. The 90% completeness limit of the survey is Ks,tot = 23.4 AB. Photometry has been determined in a color aperture by PSF matching all bands, including additional source-fitting for the large-PSF space-based imaging such as GALEX and IRAC/MIPS.

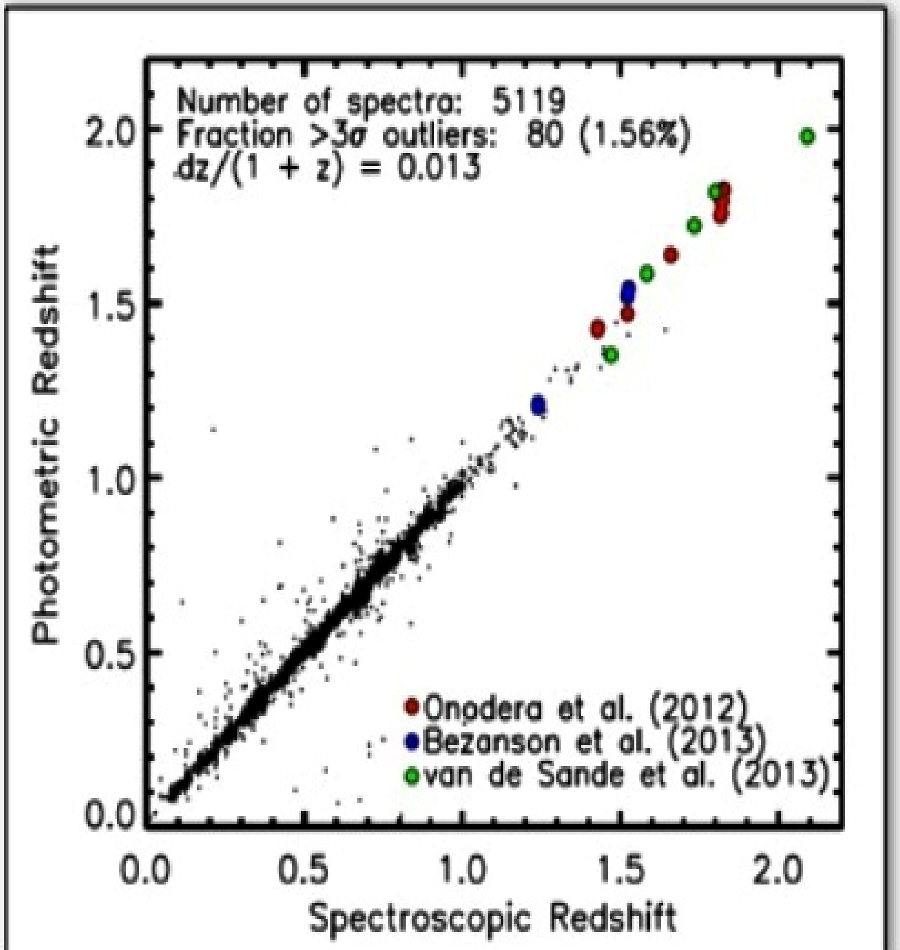

Photometric Redshifts

Photometric redshifts for galaxies have been calculated using the EAZY code. The agreement between the photometric redshifts and spectroscopic redshifts from the literature such as zCOSMOS is excellent, with an outlier fraction of 1.56% and an RMS of $dz/(1+z) = 0.013$.

3) Gravitational Lensing

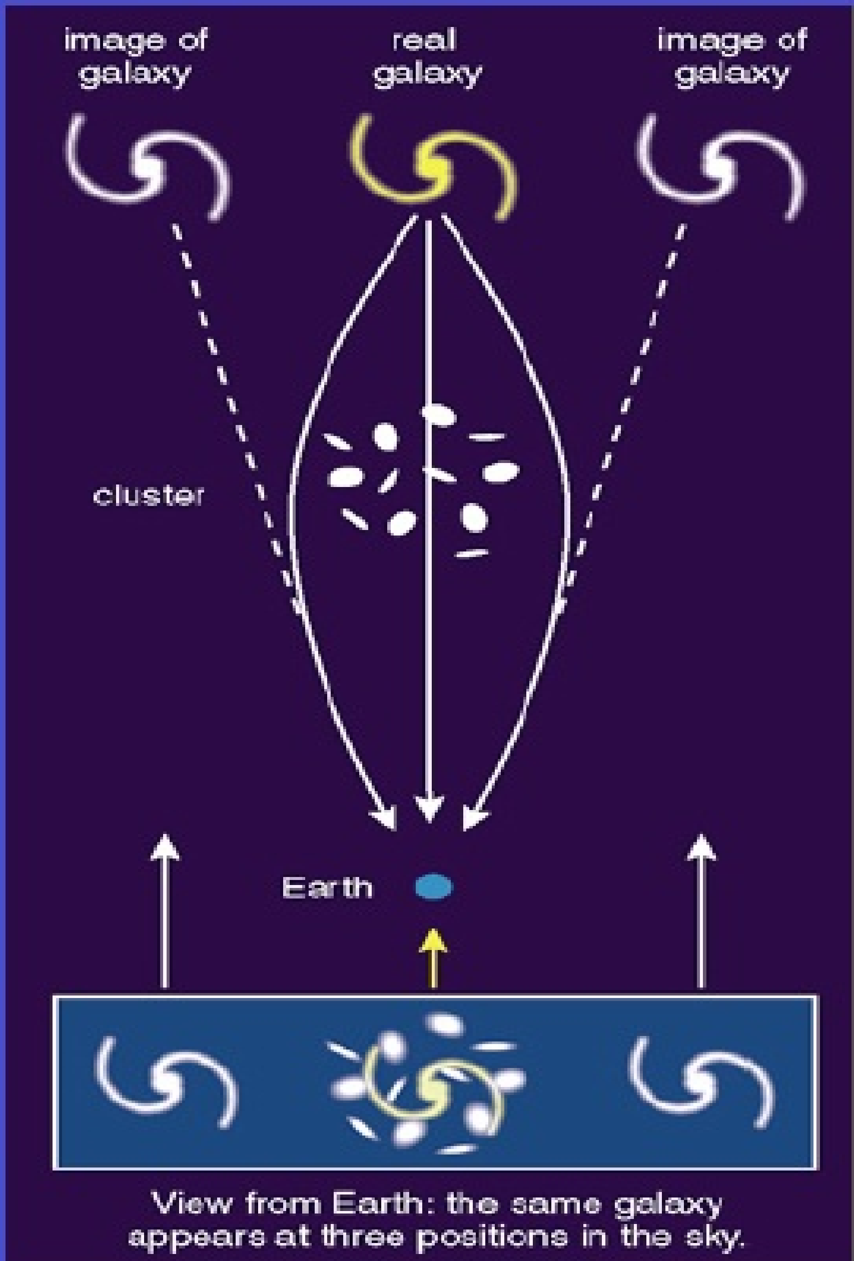

To get even more sensitivity we can add a second cosmic telescope to our ground telescope

Spitzer Detection of Lensed z~6.8 Pair

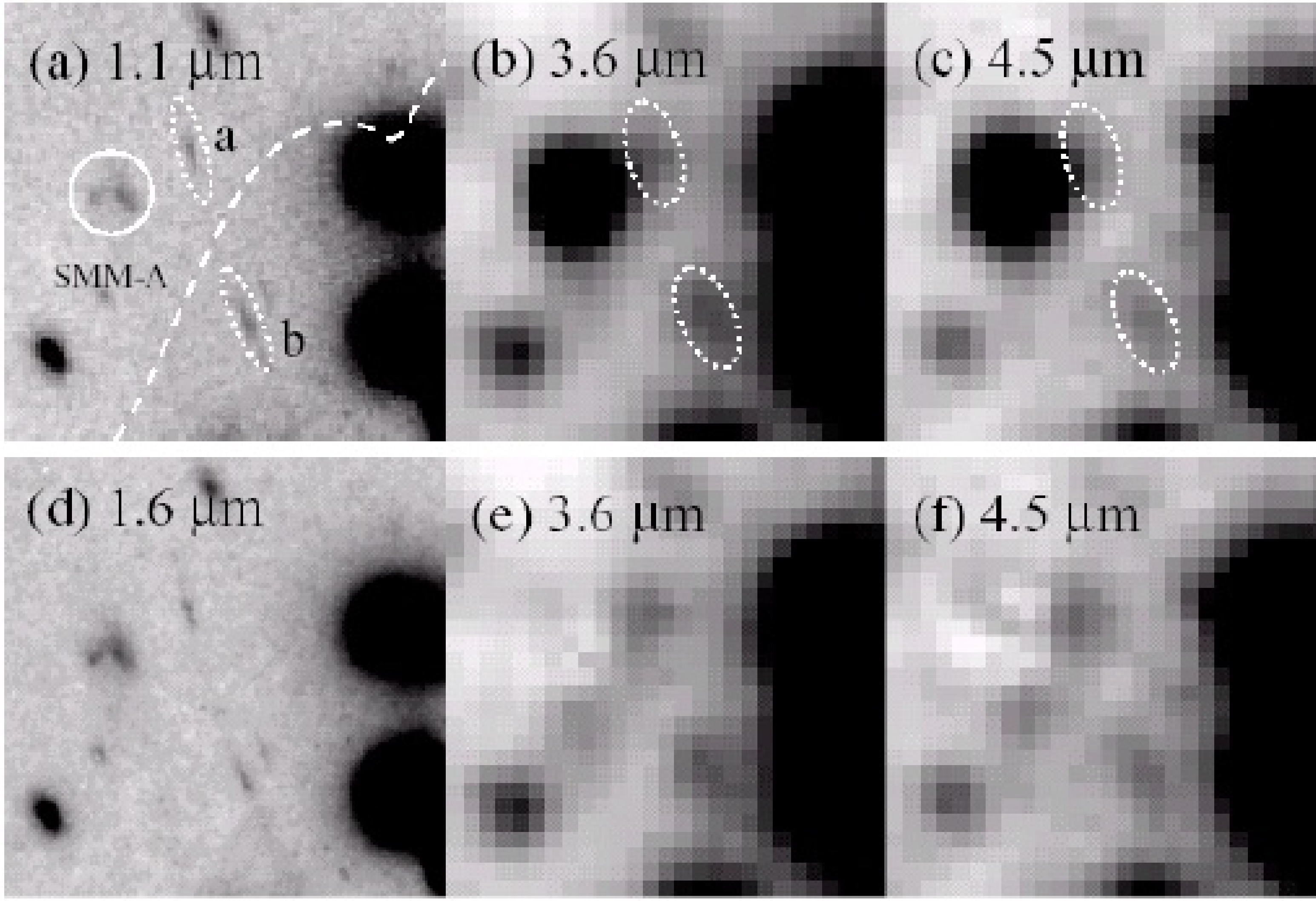

IRAC flux densities: $f_\nu(3.6\mu m) = 1.2 \pm 0.3\ \mu Jy$

$f_\nu(4.5\mu m) = 1.0 \pm 0.2\ \mu Jy$

SED Implies Established Stellar Population @ z~7

Key parameters:

SFR = 2.6 $M_\odot$ yr^{-1}

M_{star} ~ 5-10 10^8 $M_\odot$

z ~ 6.8 ± 0.1

age 40 – 450 Myr ($7 < z_F < 12$)

Age > e-folding SF time ⇒ more luminous during active phase?

(Egami et al 2005, Ap J 618, L5)

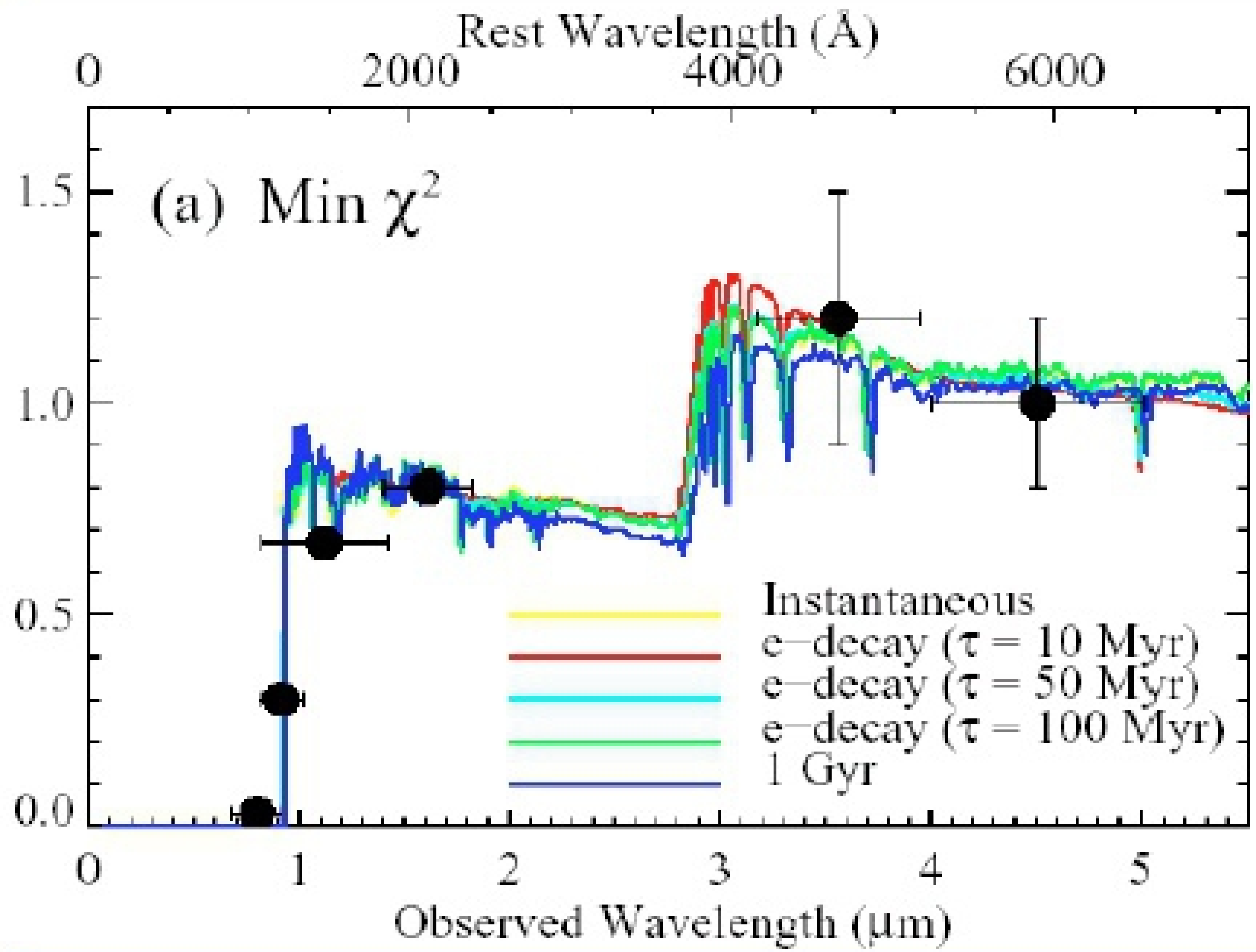

Given small search area, such sources may be very common

4) High z Lyman α Surveys

Origin: ionizing flux absorbed by H gas → Lyα photons

Efficient: < 6-7% of young galaxy light may emerge in Lα depending on IMF, metallicity etc.

1 $M_\odot$ yr^{-1} = 1.5 10^{42} ergs sec^{-1} (Kennicutt 1998)

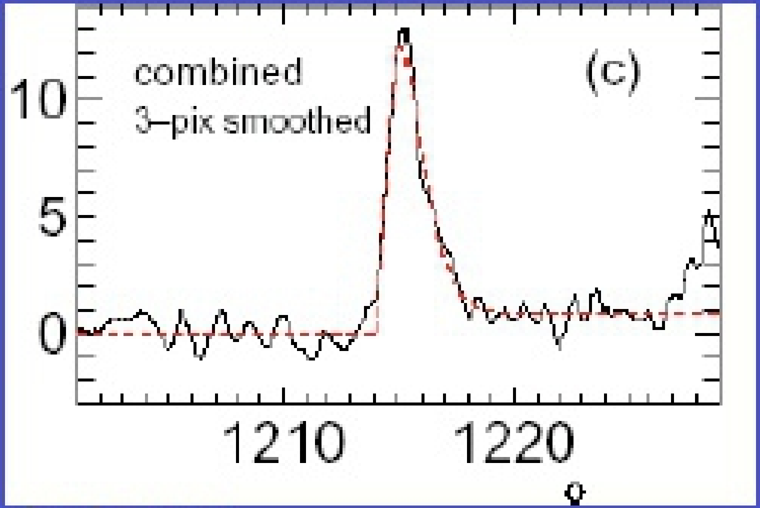

Complementary techniques:

- nb ($f_\alpha < 10^{-17}$ cgs, $L_\alpha < 5.\ 10^{42}$ cgs, SFR~3 $M_\odot$ yr^{-1}, V~2. 10^5 Mpc^3)
- lensed spectra ($f_\alpha < 3.10^{-19}$, $L_\alpha < 10^{41}$, SFR~0.1 $M_\odot$ yr^{-1}, V <50 Mpc^3)

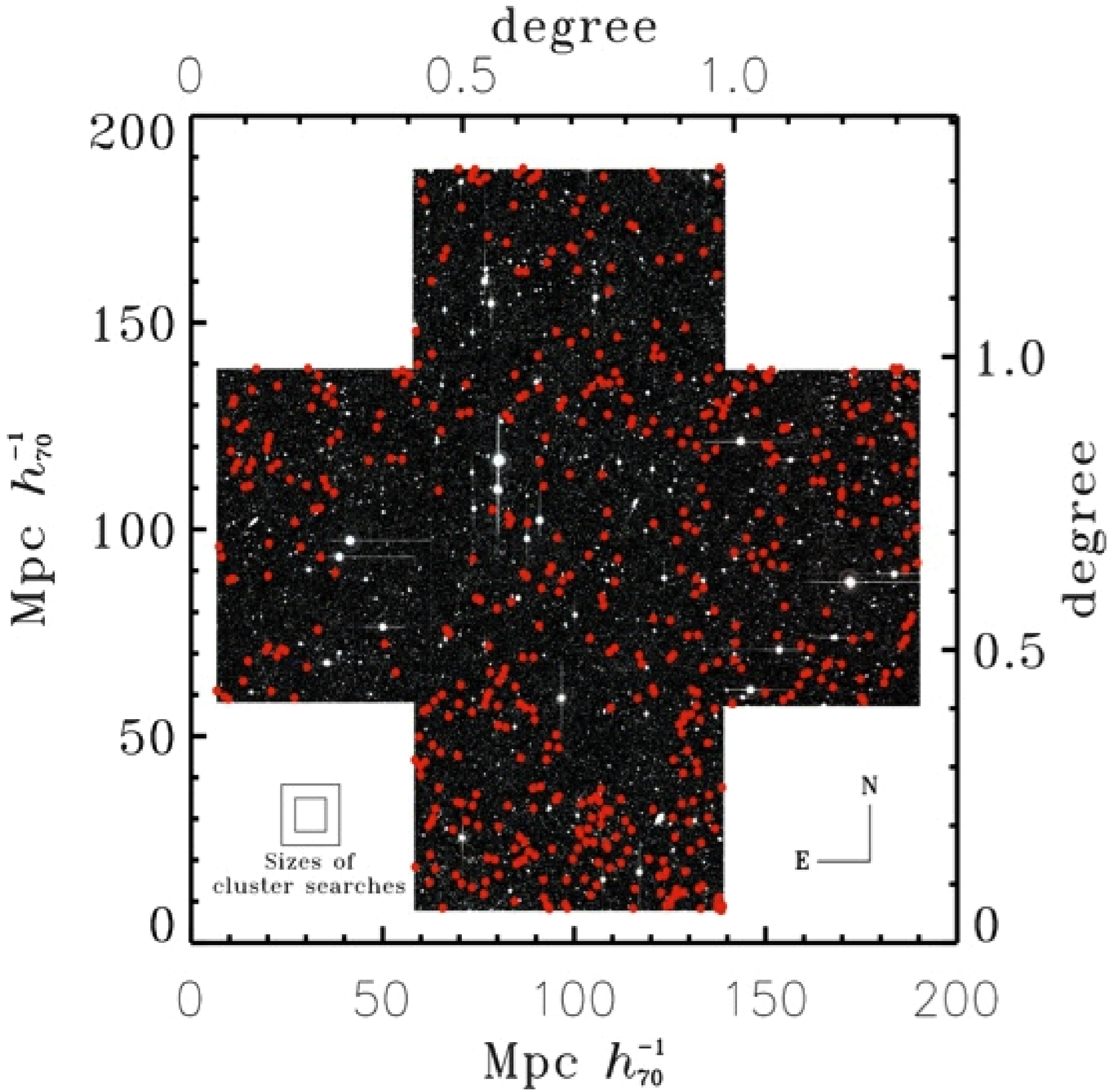

\scriptsize{9} {\bf Lyman Alpha Emitters at redshift $z = 5.9$} Red dots show the locations of Lyman Alpha Emitter candidates detected in narrowband-wideband image ratios. Large Scale Structure is apparent in the form of clusters and voids in the LAE locations. Plot from Ouchi et al. (2005) \protect \cite{ouchi05}, adapted by Kevin Bandura

5) Sub-mm galaxies

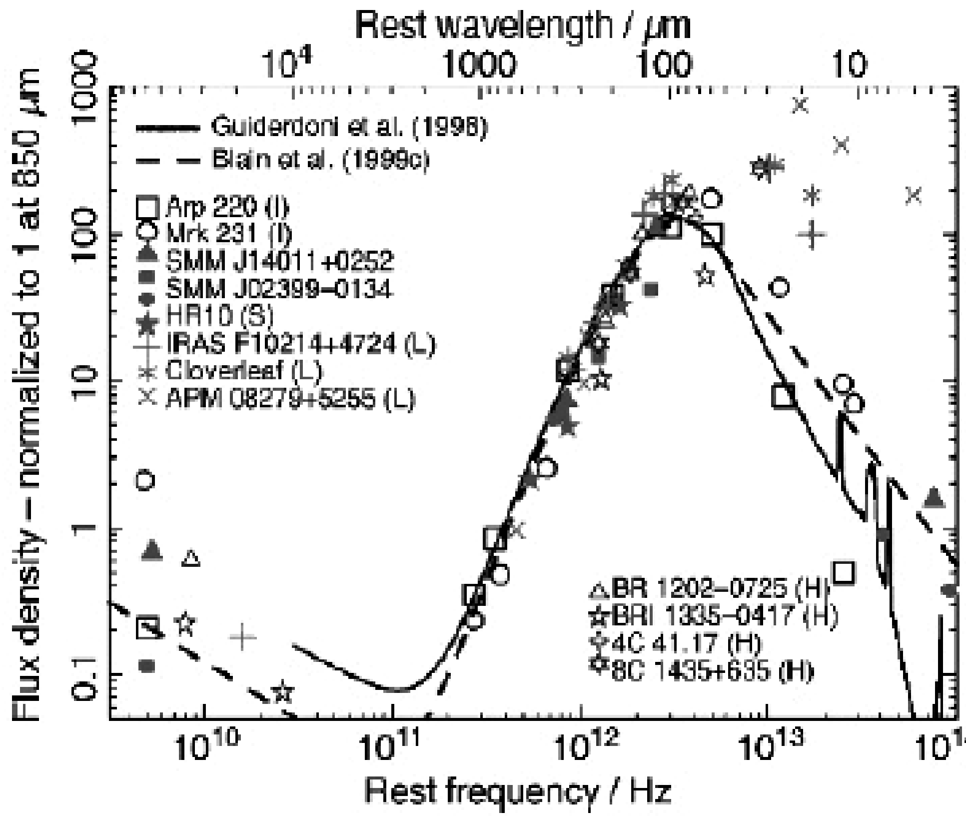

- Sub-mm telescopes (SCUBA) operating at 0.4-1.3 mm mainly see dust at 20-40 K.
- Spectrum $S_\upsilon \sim \upsilon^{2+\beta}$ with $1 < \beta < 2$. Redshift increases rest-frame υ and increasing spectrum leads to a negative K-correction.
- For $z_{max} > z > 1$, flux stays constant or increases.
- What sets z_{max}? For dust at 40 K and $\lambda \sim 0.85$ mm, $z_{max} \sim 8$.

Sub-mm galaxies

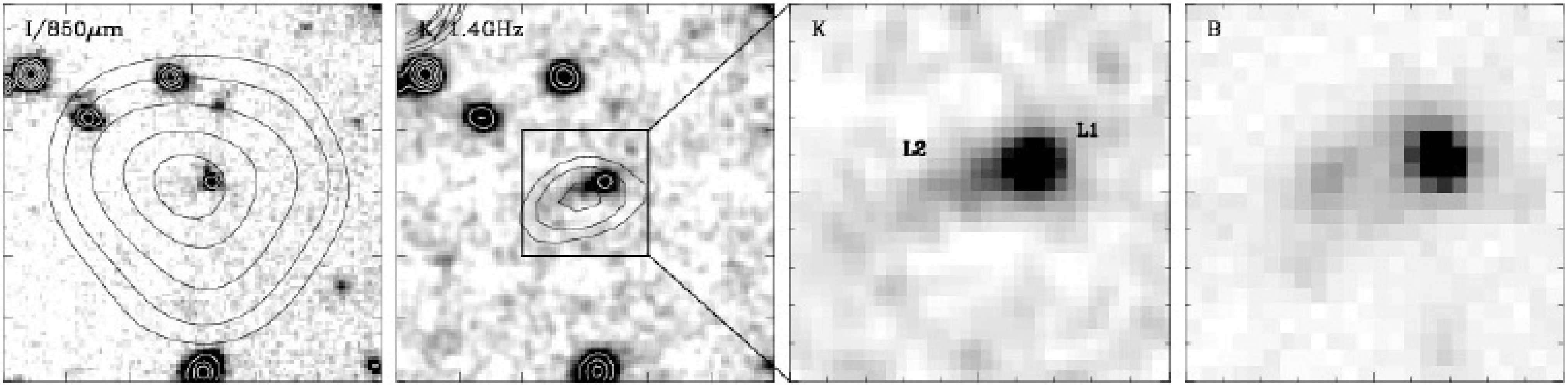

- SCUBA positions good to ~15" making optical identification difficult.
- Counterparts identified in radio with VLA (1.4 GHz, 1") and then in optical.
- Redshifts from optical or a sort of photo-z from radio/sub-mm flux ratio.
- Median $z \sim 2.5$. Galaxy masses $\sim 10^{11}\ M_{Sun} \sim 10\times$ mass of LBGs.
- From mass, number density, and optical morphology, sub-mm galaxies are thought to be ellipticals in the process of formation.
- Many sub-mm have AGN revealed in X-rays, but X-ray/sub-mm ratio is low suggesting galaxies are dominated by star formation.

What are the main things learned from empirical studies of high redshift galaxies?

LOWER-LUMINOSITY GALAXIES COULD REIONIZE THE UNIVERSE: VERY STEEP FAINT-END SLOPES TO THE *UV* LUMINOSITY FUNCTIONS AT $z \geq 5$–8 FROM THE HUDF09 WFC3/IR OBSERVATIONS*

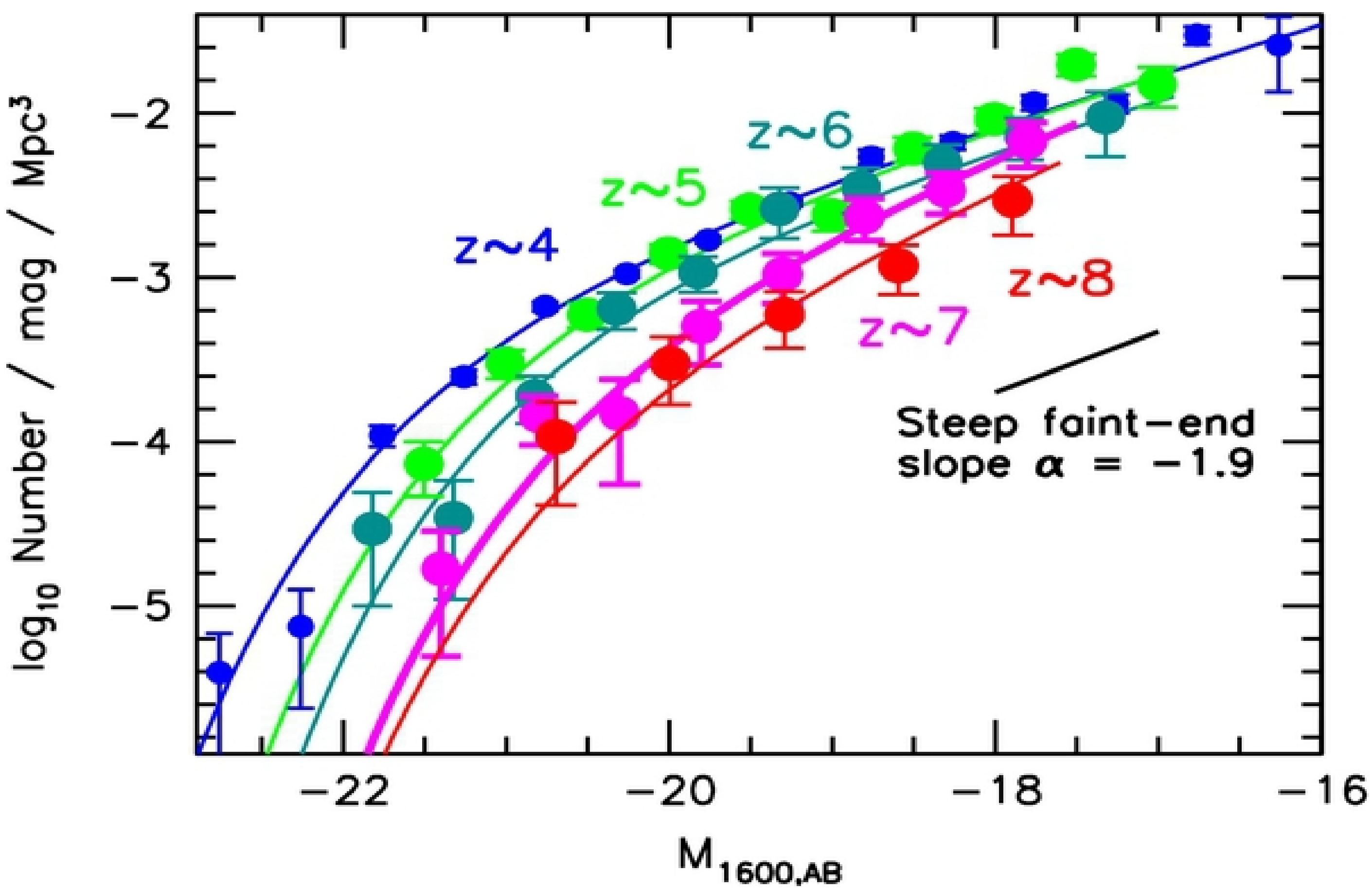

We compute the time evolution of the filling factor of ionized hydrogen $Q_{\mathrm{H\,II}}$ using the following relation we adapted from Madau et al. (1999):

where f_{esc} is the escape fraction of Lyman-continuum photons into the intergalactic medium (IGM), n_{H} corresponds to the comoving volume density of neutral hydrogen in the universe, t_{rec} corresponds to the recombination time for neutral hydrogen, and $\rho(\mathrm{SFR})_{\mathrm{uncorr}}(z)$ is the star formation rate (SFR) density uncorrected for dust extinction. In deriving the SFR density, we integrate the LF down to -10 mag, given the likely suppression of galaxy formation at smaller scales from the UV background, SNe feedback, and inefficient gas cooling (e.g., Read et al. 2006; Dijkstra et al. 2004).

To account for the increased ionizing efficiency (by up to 30%) of low metallicity stars expected to make up galaxies in the early universe, we assume $10^{53.2}$ photons s^{-1} per $M_{\odot}\ \mathrm{yr}^{-1}$ (Schaerer 2003). We take f_{esc} to be $\sim$20% motivated by the observations of Shapley et al. (2006) and Iwata et al. (2009), but acknowledge that f_{esc} is still very poorly determined at $z \sim 2$–3

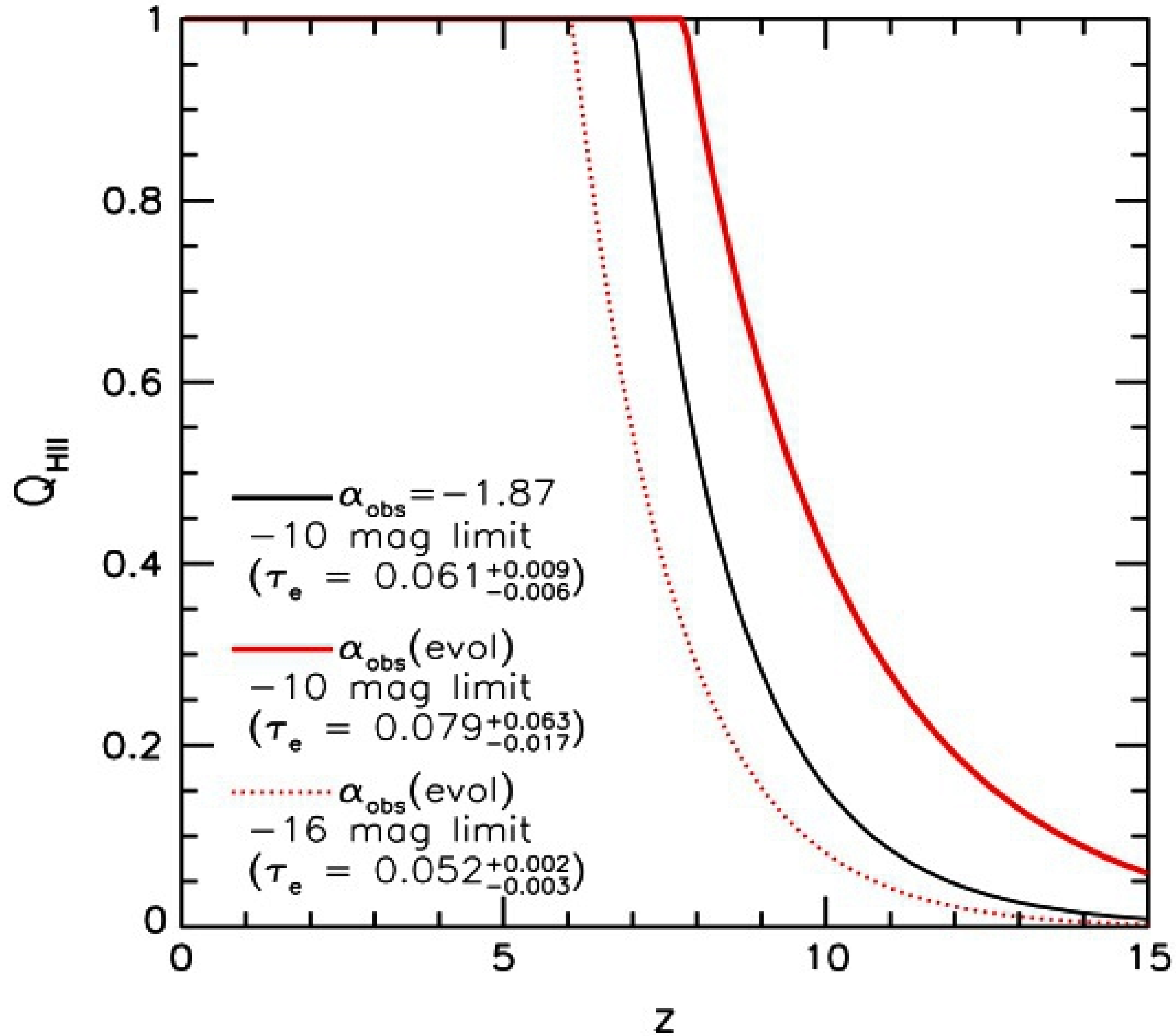

Figure 3. Filling factor of ionized hydrogen $Q_{\rm H\,II}$ vs. redshift using our LF-fitting formula for *UV* LF at $z \geqslant 4$ (Table 1). The respective ionization histories (represented by the lines) were calculated from Equation (2) assuming a Lyman-continuum escape fraction $f_{\rm esc}$ of 20%, a clumping factor of three, an IGM temperature of 2×10^4 K, a $1/50\ Z_\odot$ Salpeter initial mass function, and assuming the LF extends down to −10 mag (with the same faint-end slope α). See the

Rise and fall of the integrated star formation rate density in galaxies, with a peak at redshifts 2-3

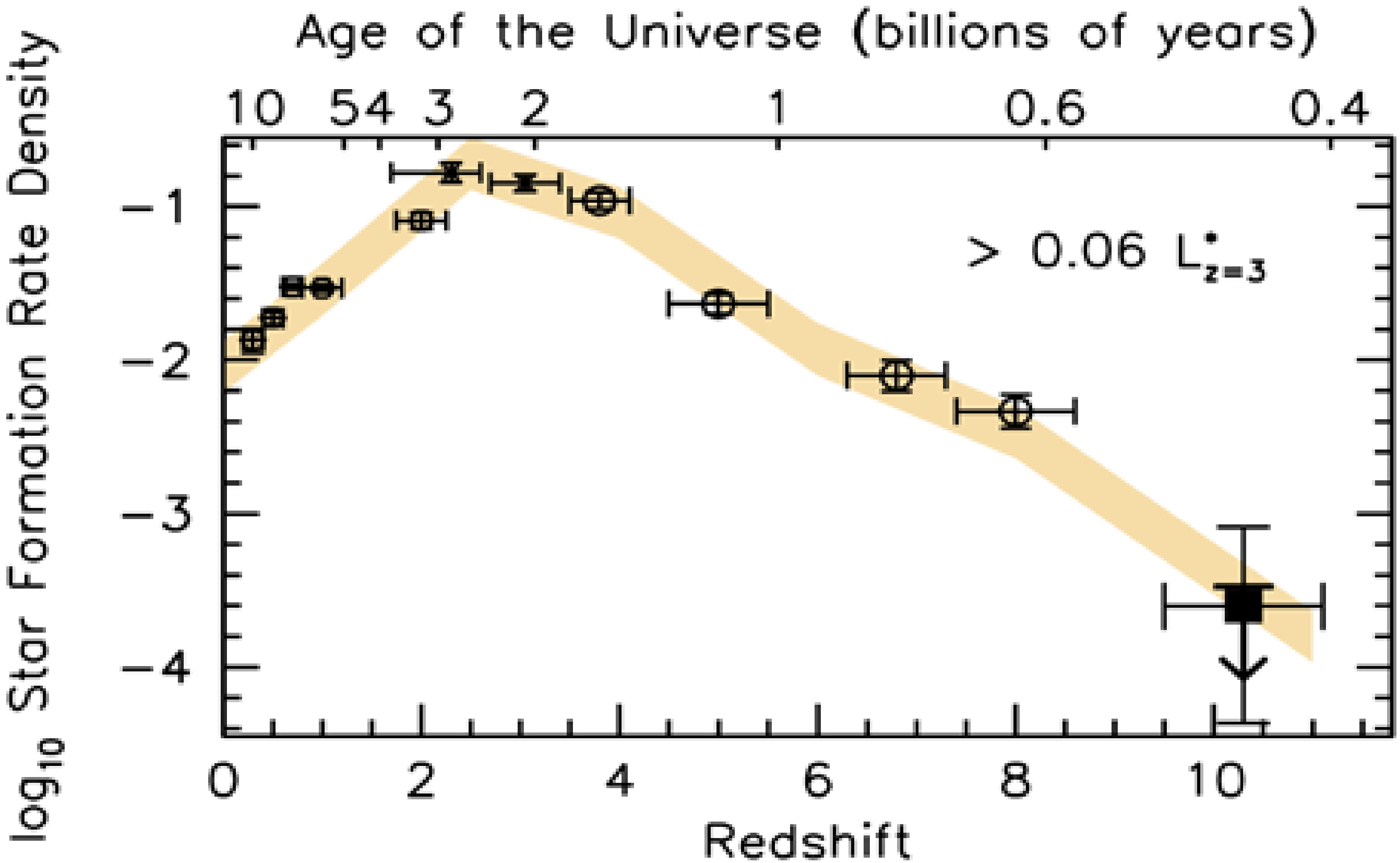

Buildup of the cosmic density of stars in galaxies

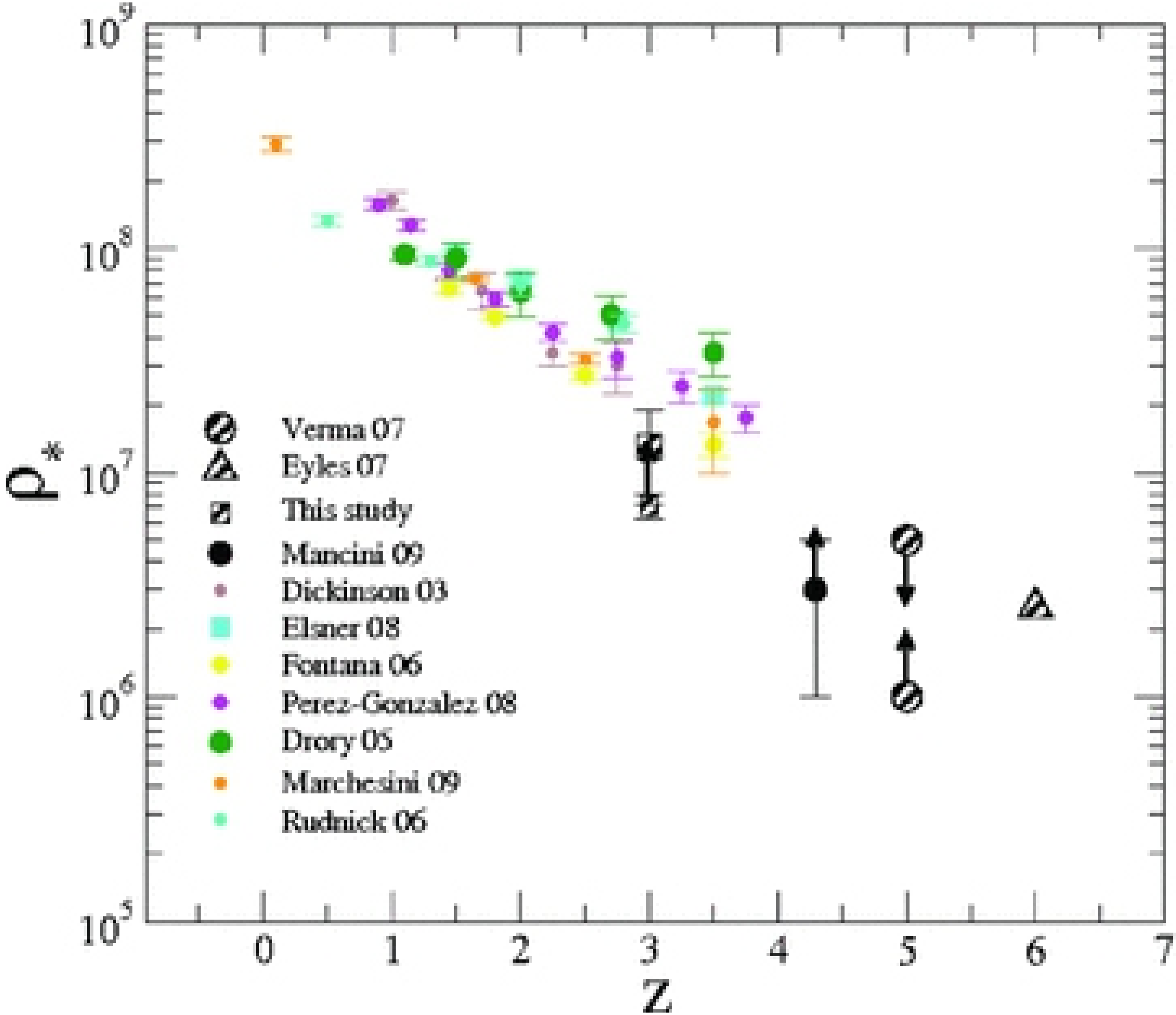

Evolution of the Stellar Mass Function to High Redshifts (note recent rapid evolution at low mass end)

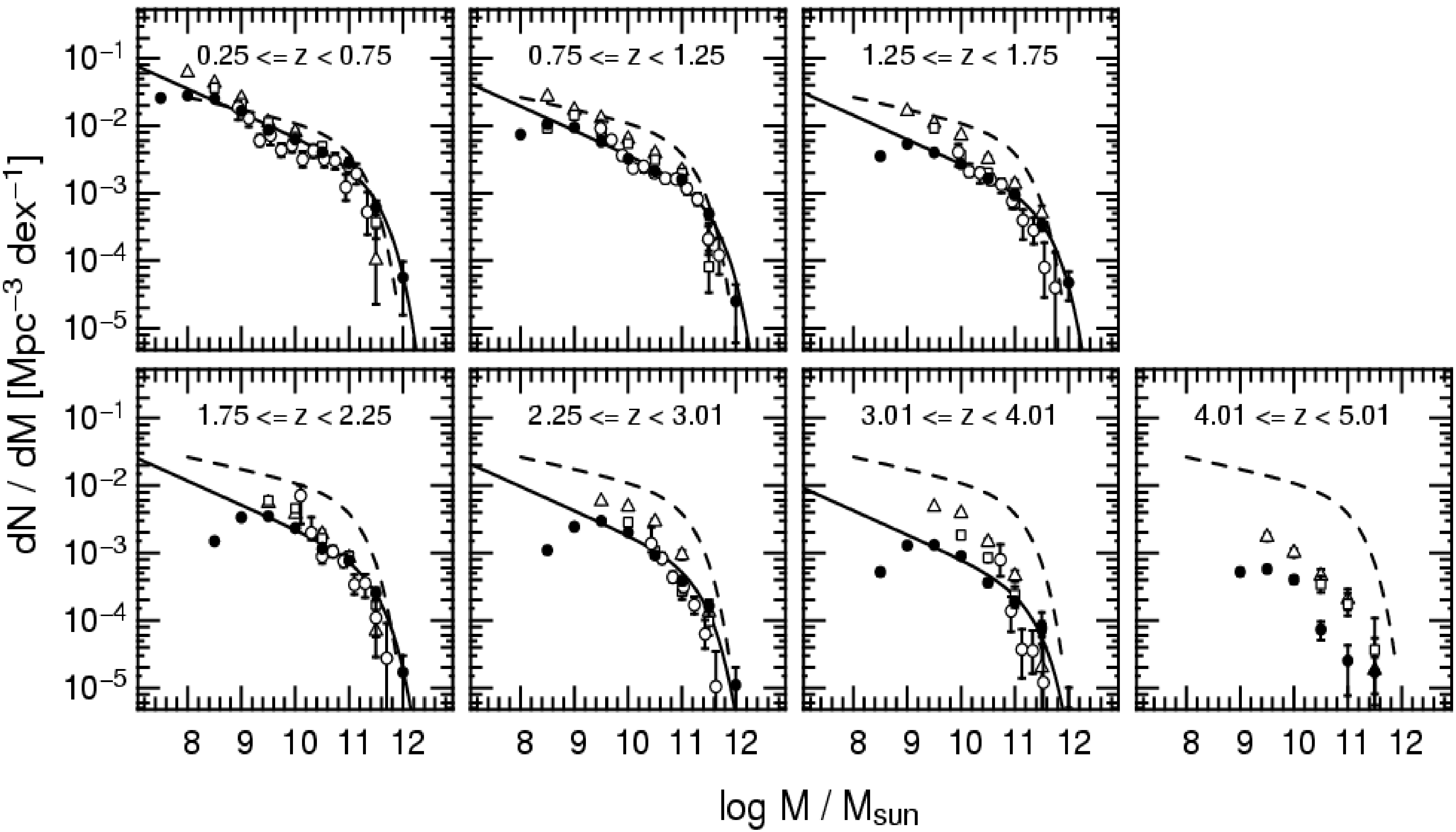

This is consistent with the star formation histories of galaxies as a function of mass inferred from studying their stellar populations at low redshifts

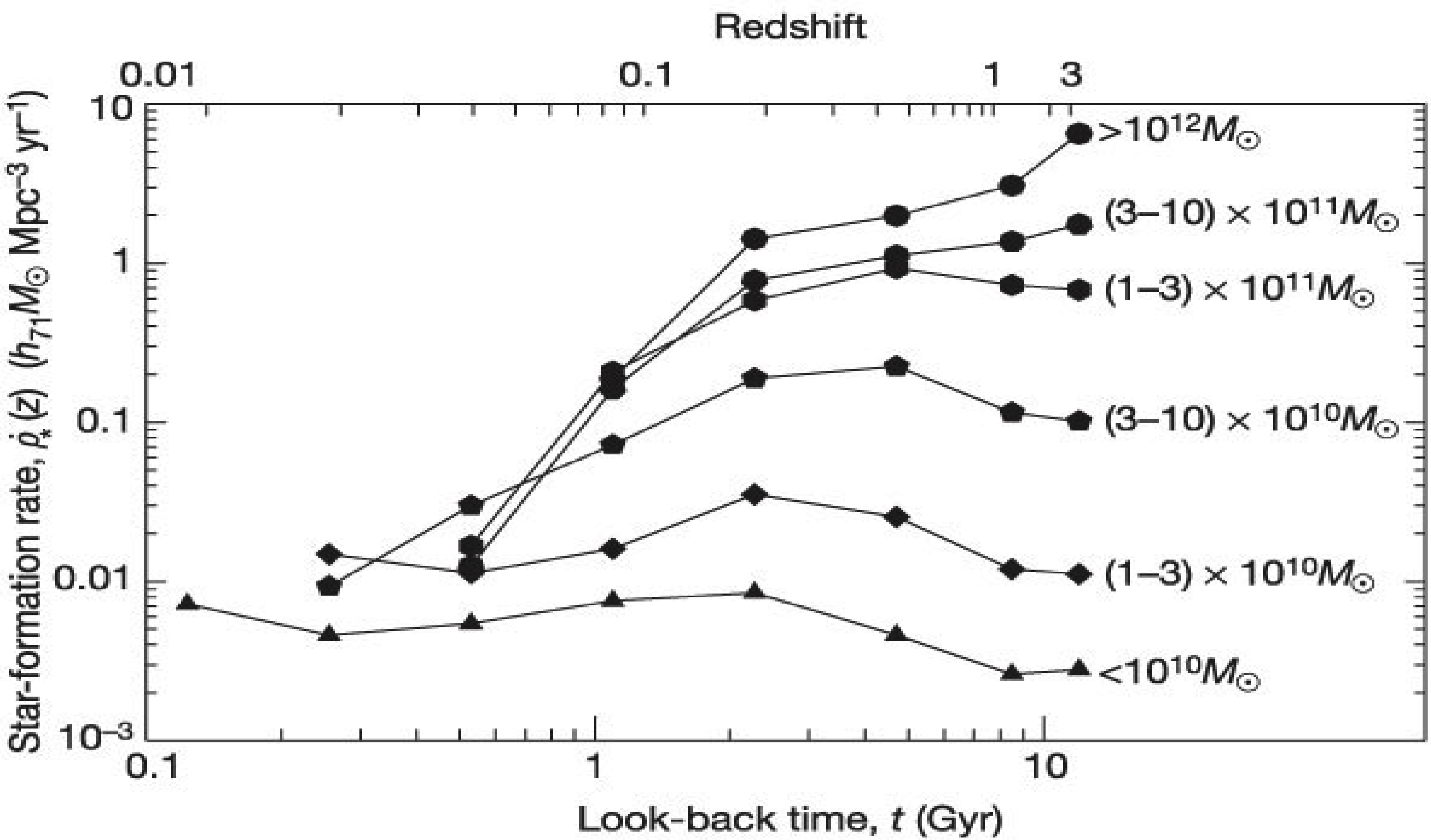

Colour Bimodality in Galaxy Population at z=0

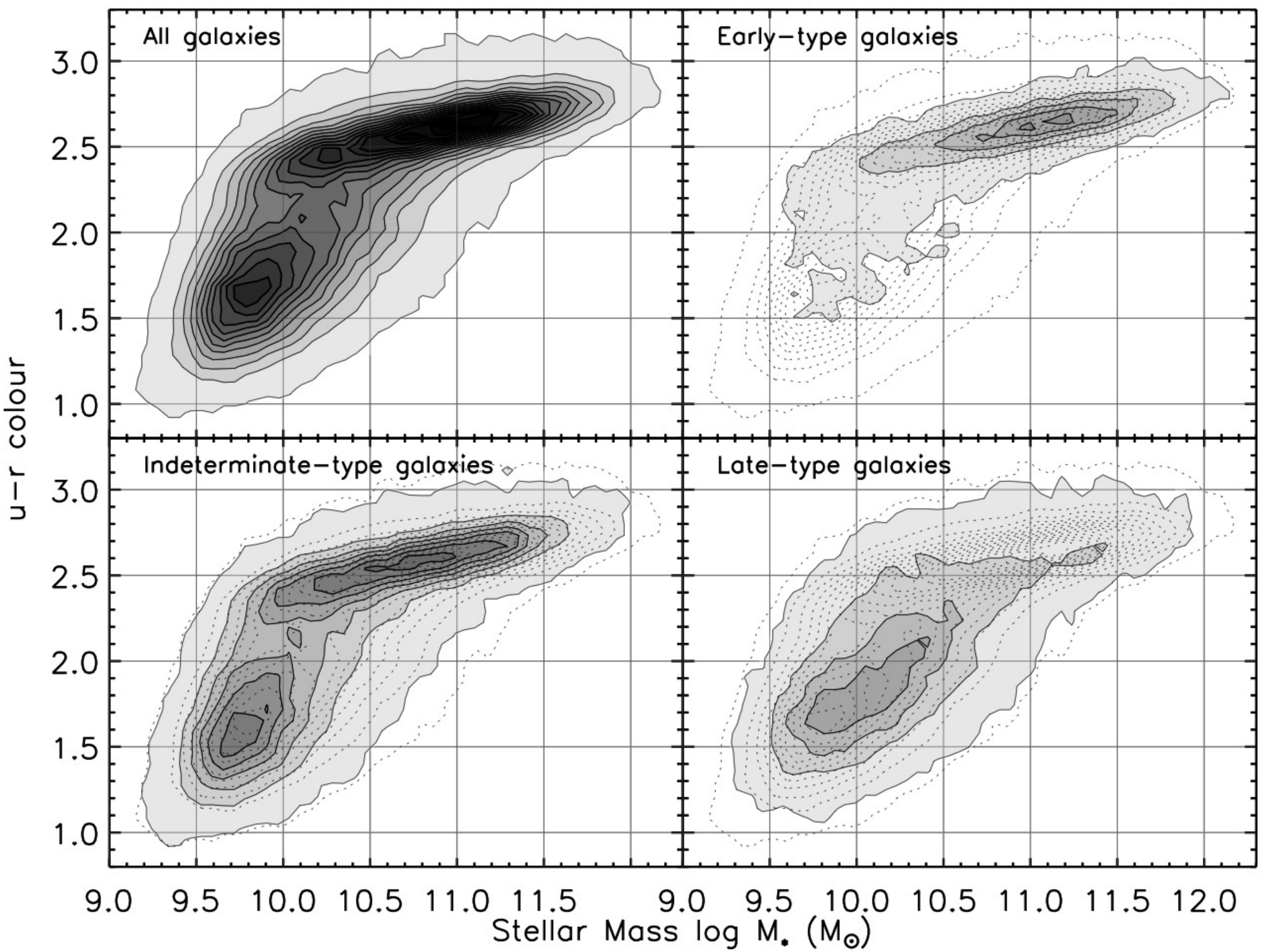

Bimodality persists at higher redshifts

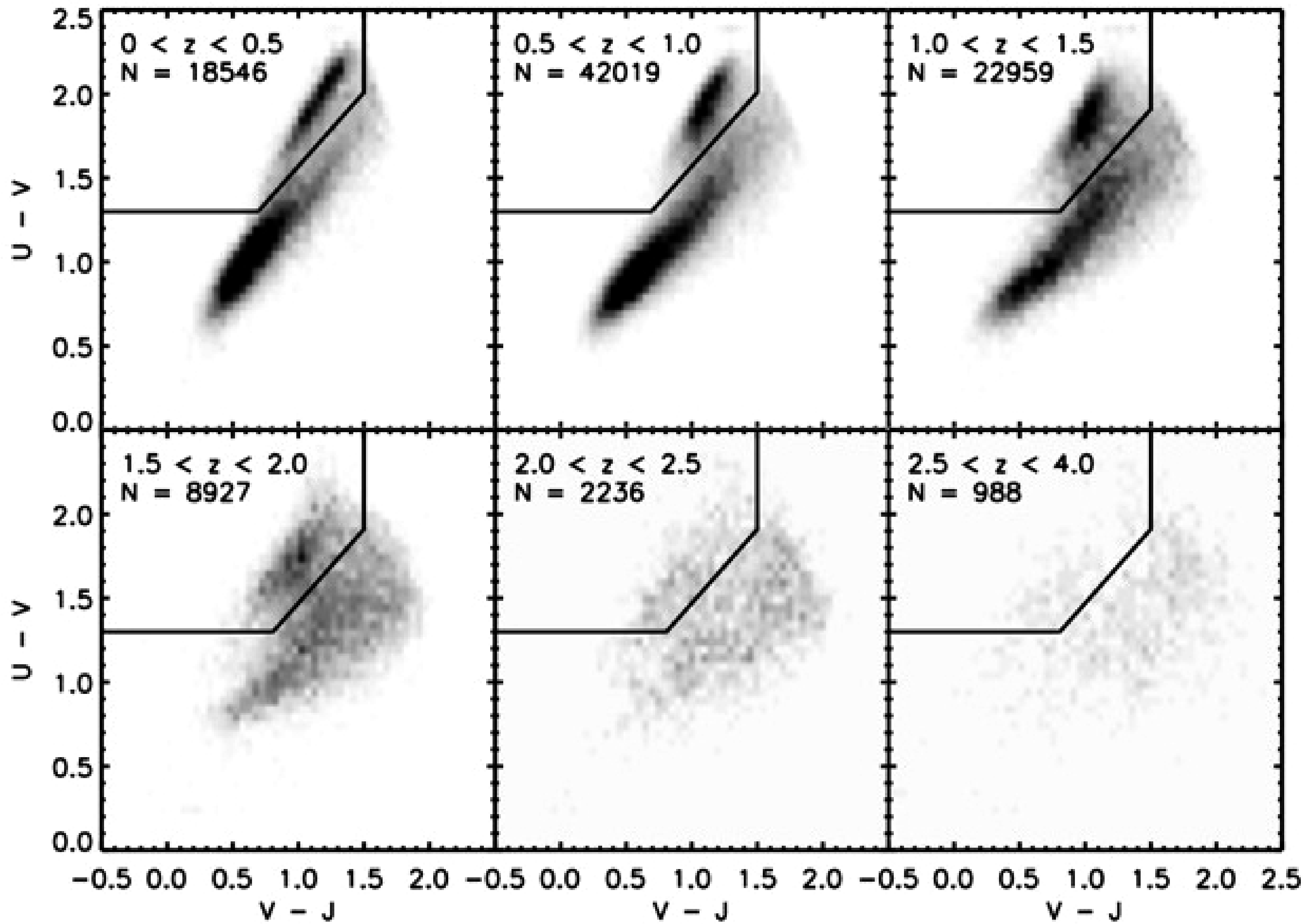

FIG.1. UVJ color-color diagram at various redshifts for galaxies more massive than the 95% mass-completeness limits. The bimodality in the galaxy population is clearly visible up to z=2. The cuts used to separate star forming from quiescent galaxies for the SMFs are shown as the solid lines.

Stellar mass density in the red sequence drops faster than that in the blue cloud

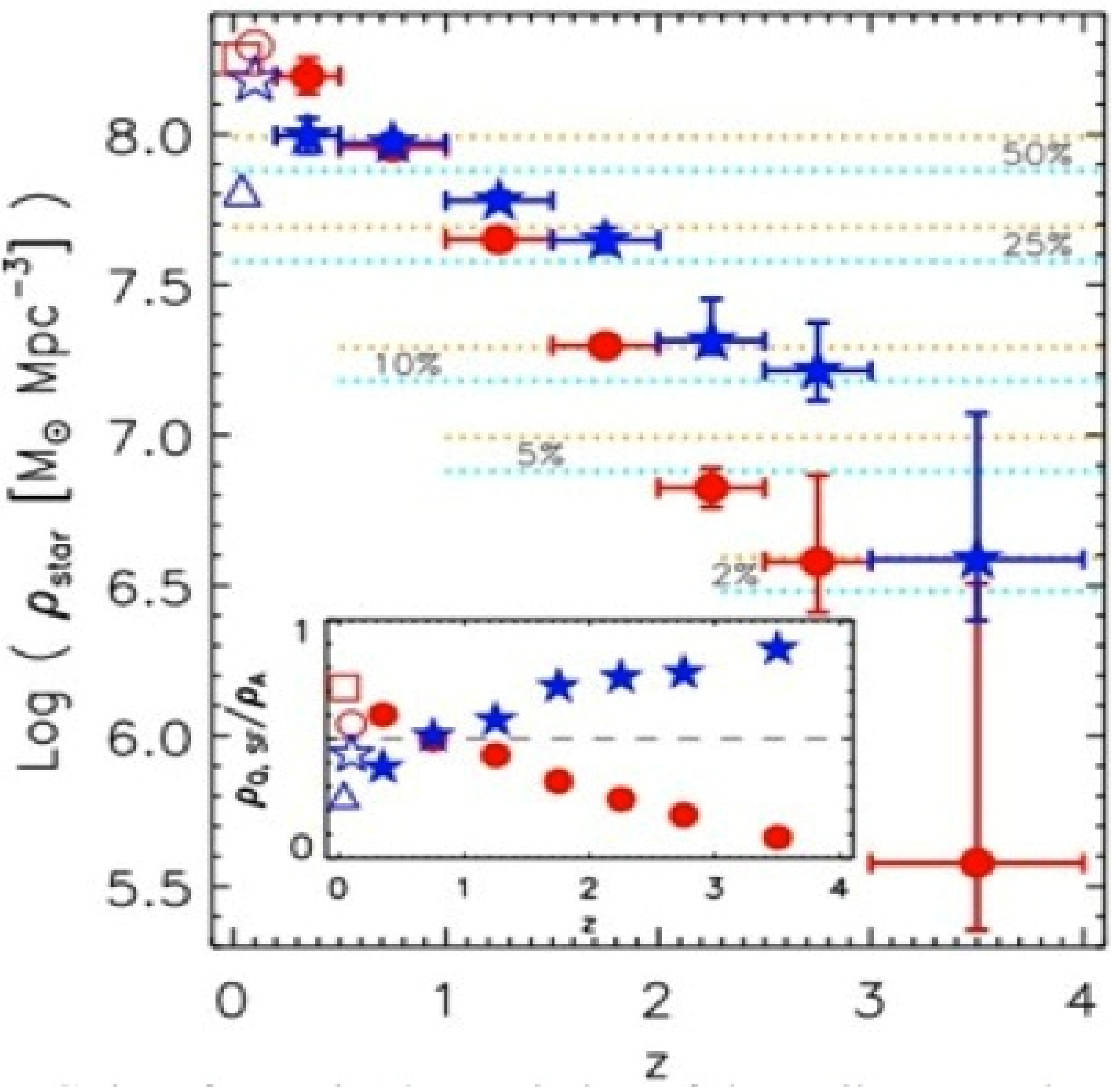

Most of the evolution is at the low mass end for both classes....

Stellar Masses

Stellar masses and other population parameters are calculated for all galaxies using the FAST code. These are determined from fitting the SEDs of the galaxies to models such as Bruzual & Charlot (2003) and Maraston (2005). FAST also outputs stellar population parameters such as ages and star formation rates. All of the best-fit SEDs from the FAST fits are available in the data products page.

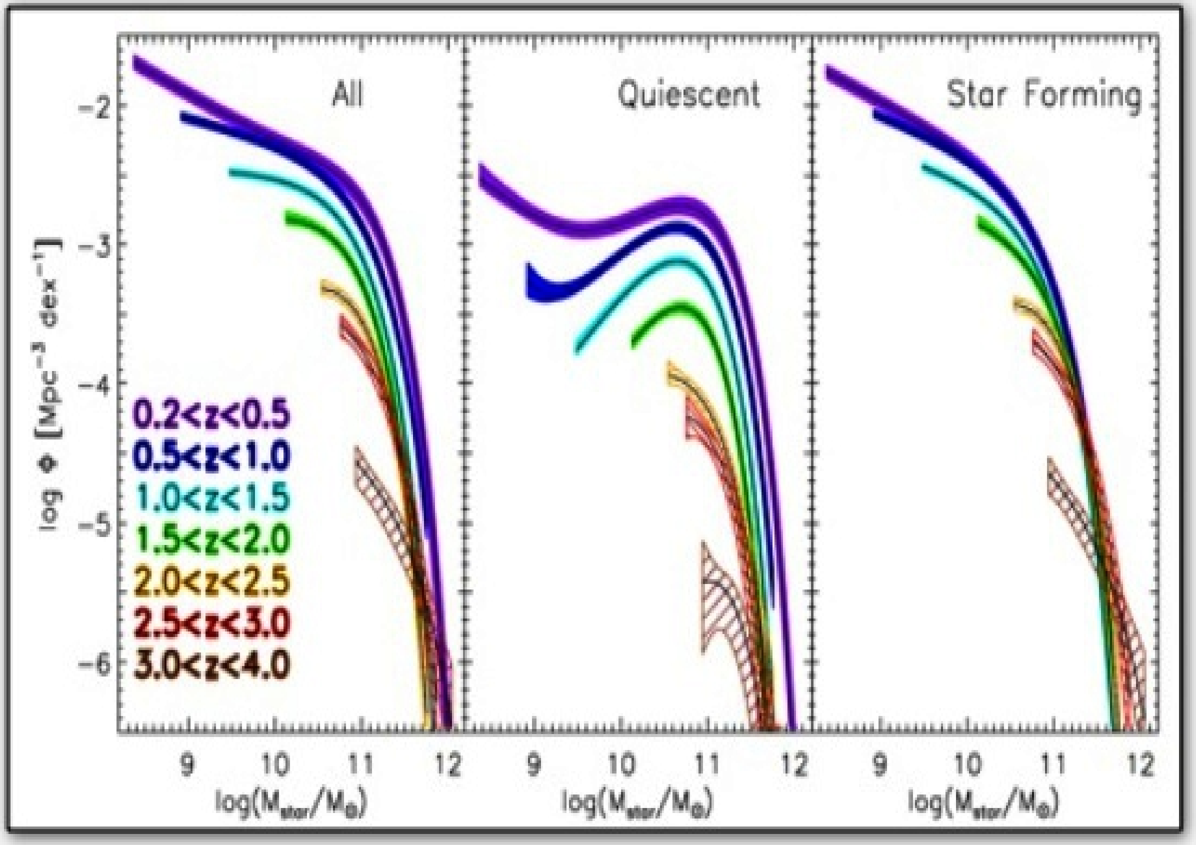

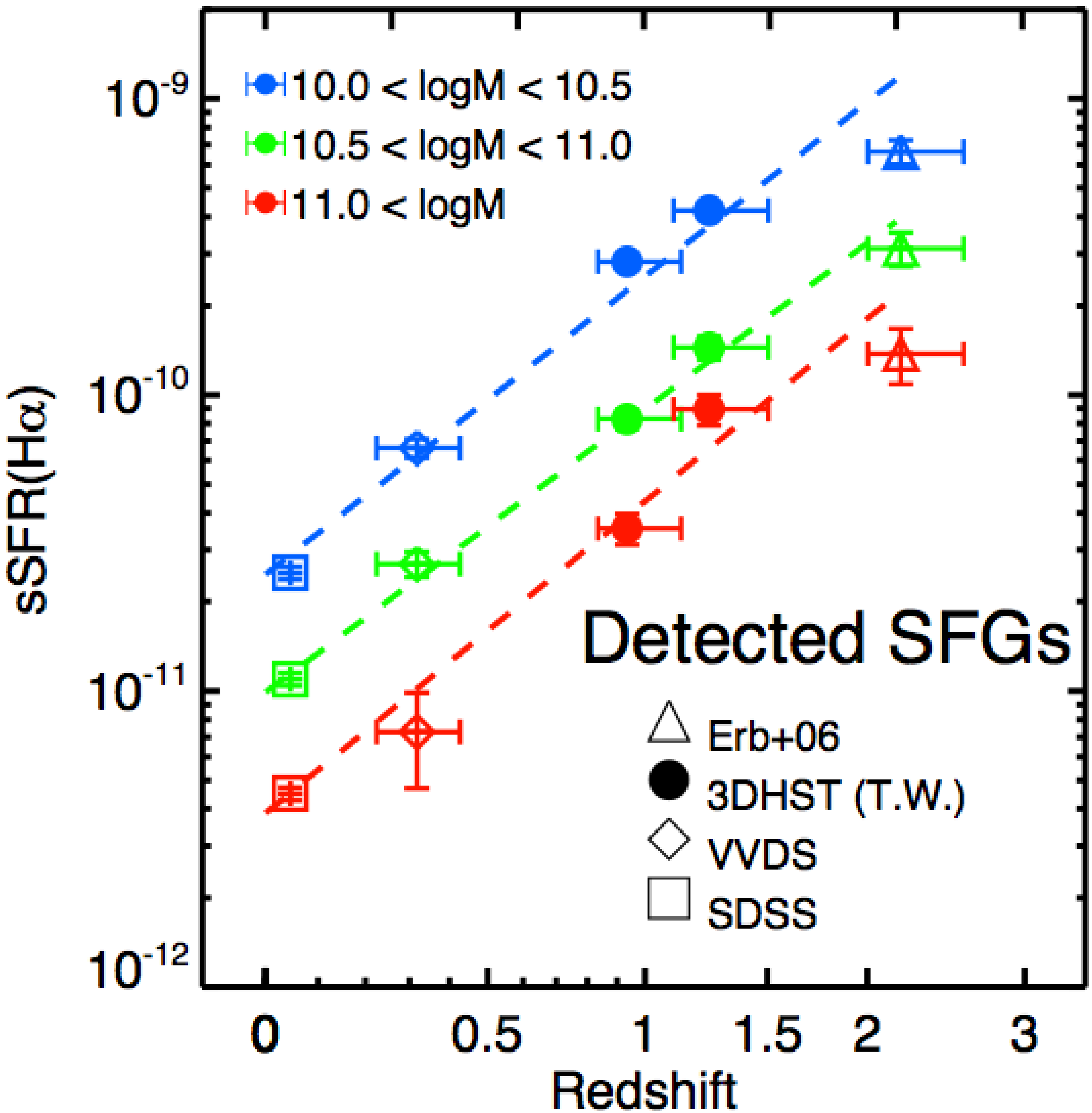

Evolution in star formation rate per unit mass (specific SFR) for star-forming galaxies

At fixed stellar mass, the gas metallicities of galaxies are lower at higher redshifts

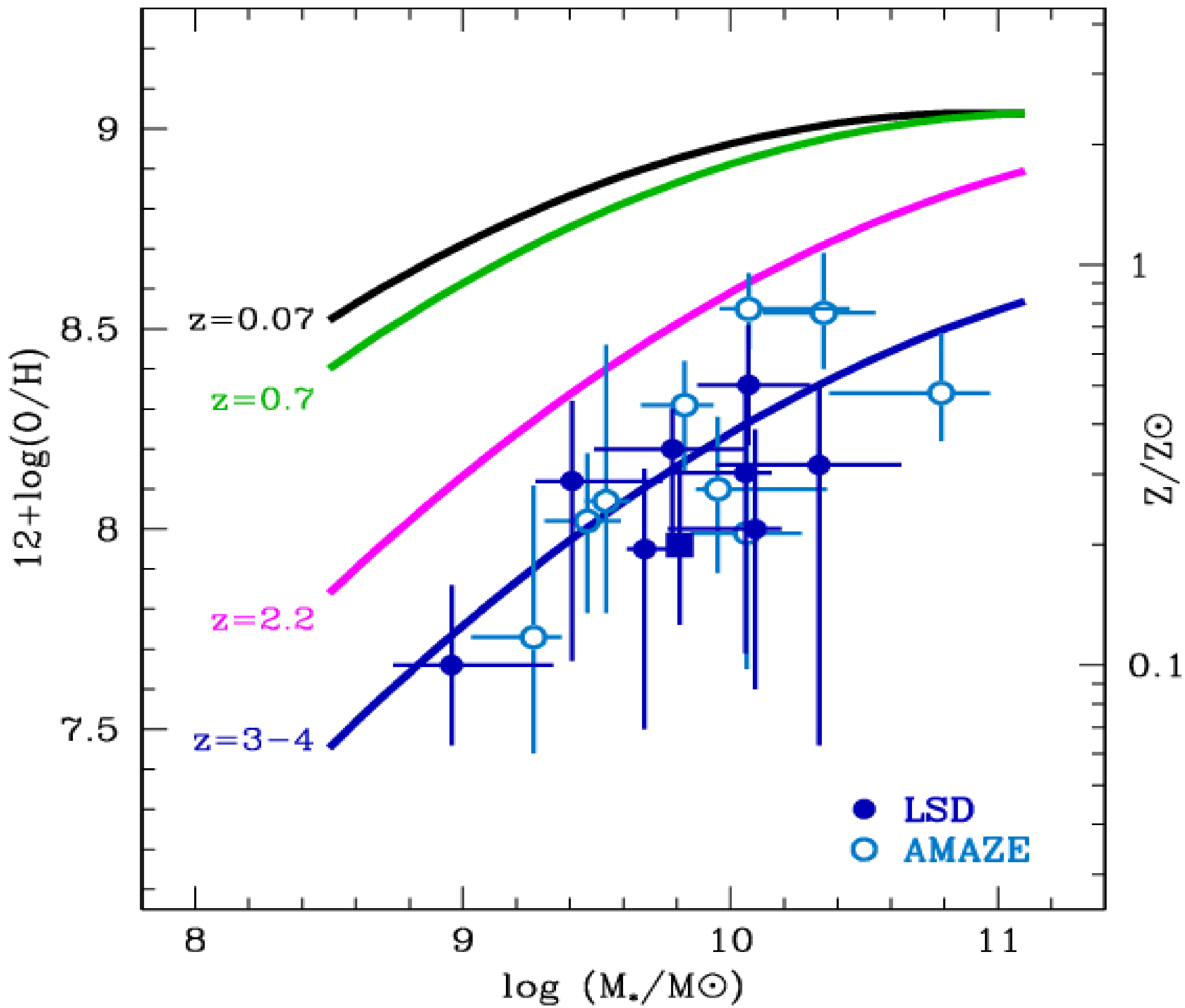

High redshift star-forming galaxies have clumpier morphologies than nearby spiral galaxies

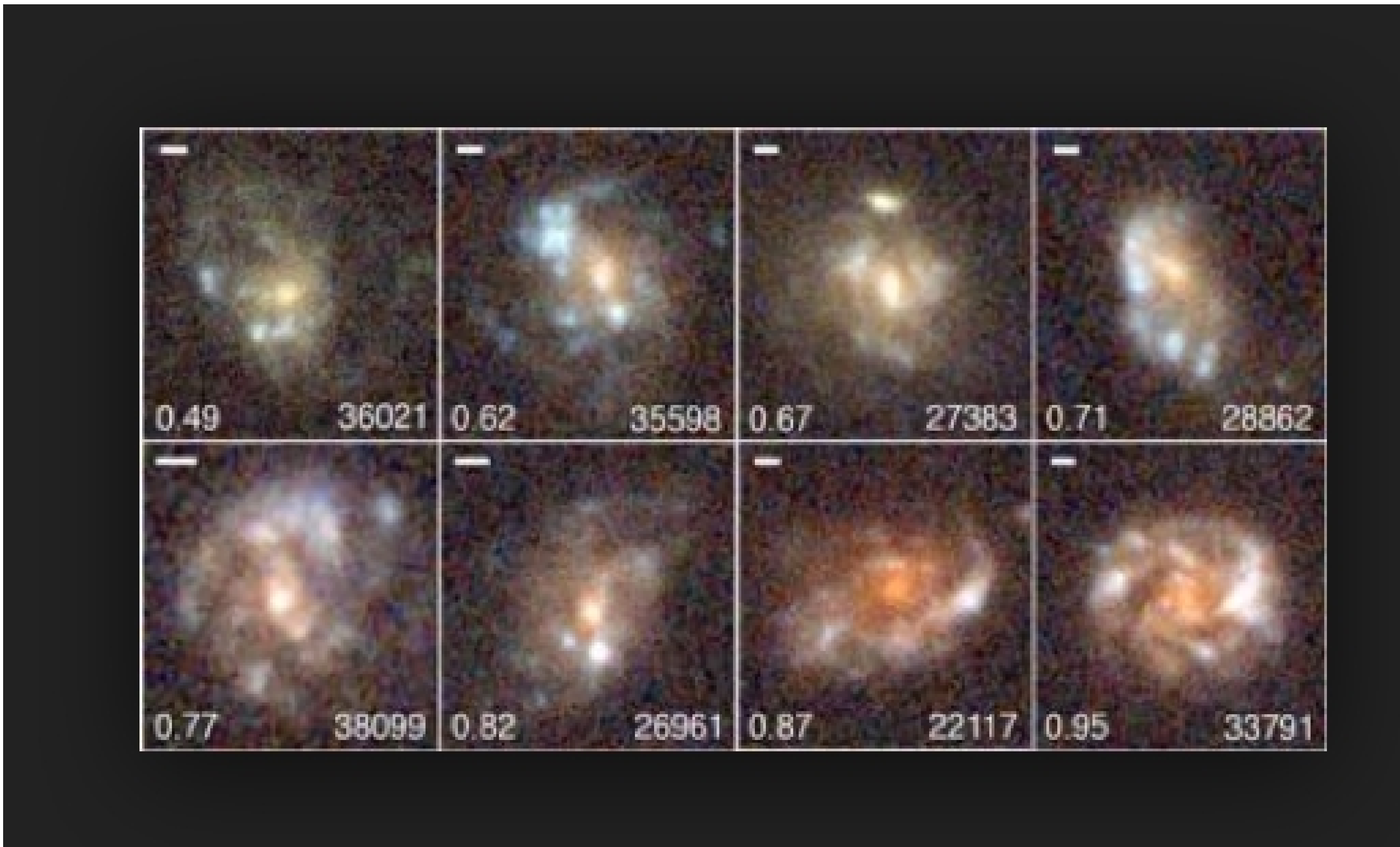

These giant clumps of young stars drive outflows of gas – in the high redshift Universe, this is a UBIQUITOUS phenomenon (at low redshifts, much more rare)

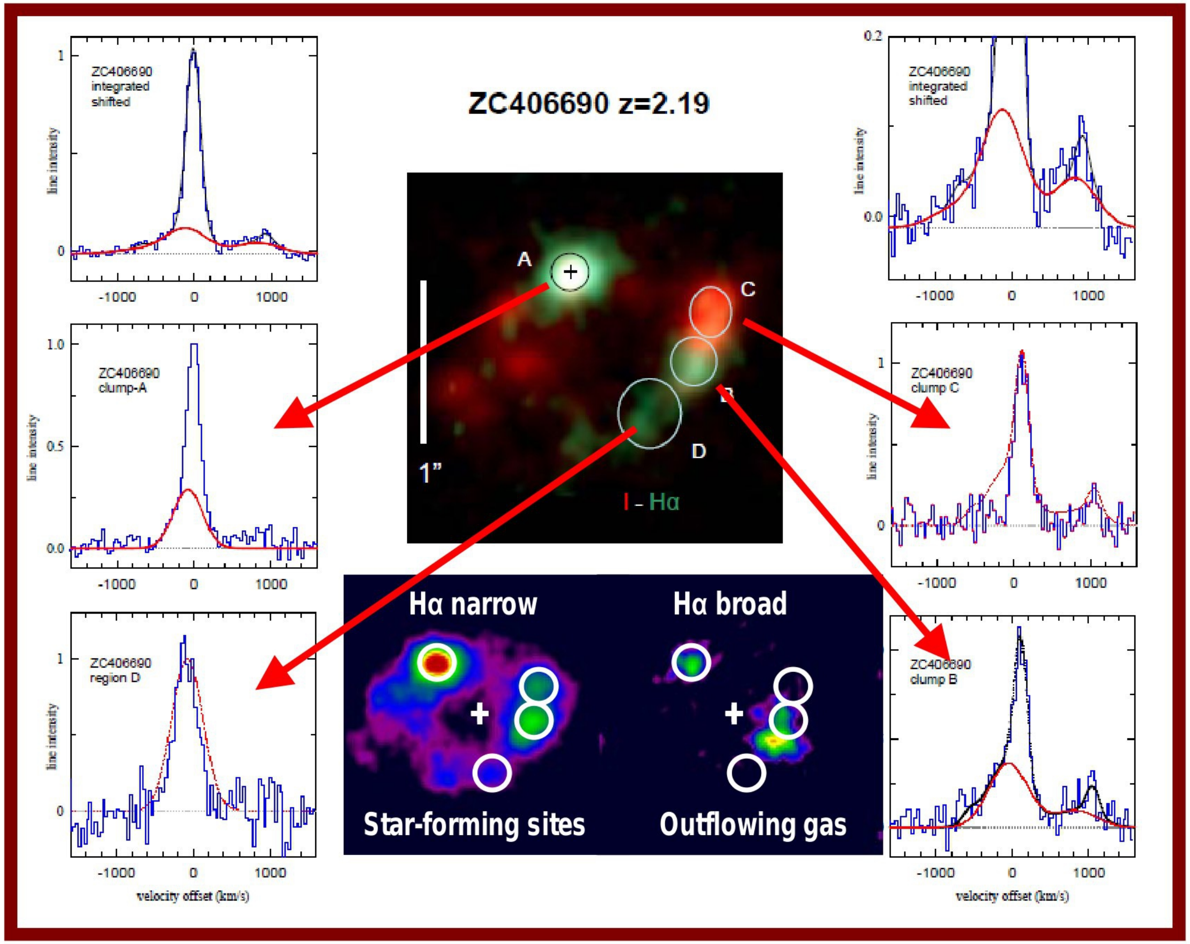

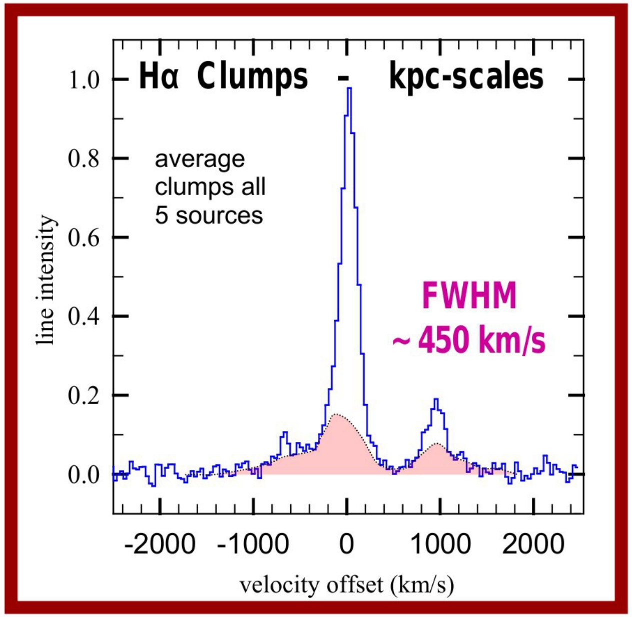

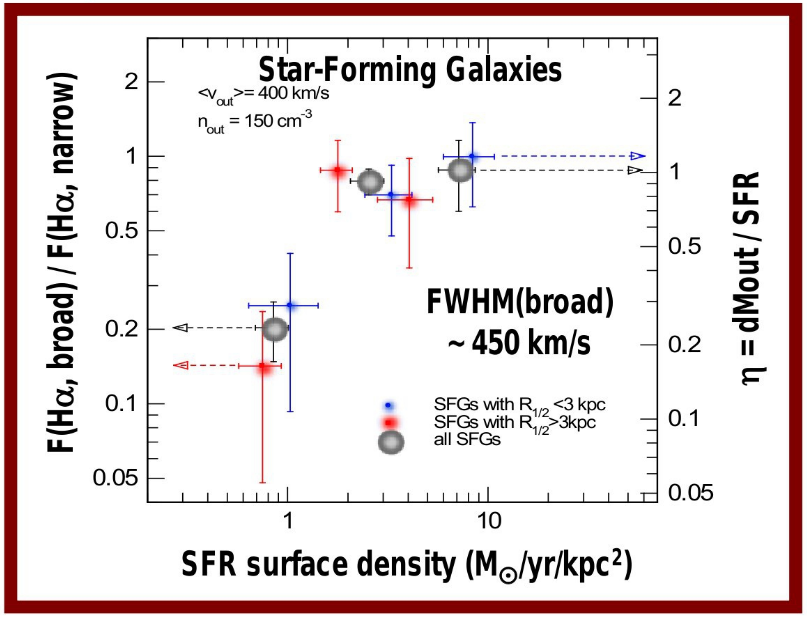

Outflows traced by interstellar absorption lines

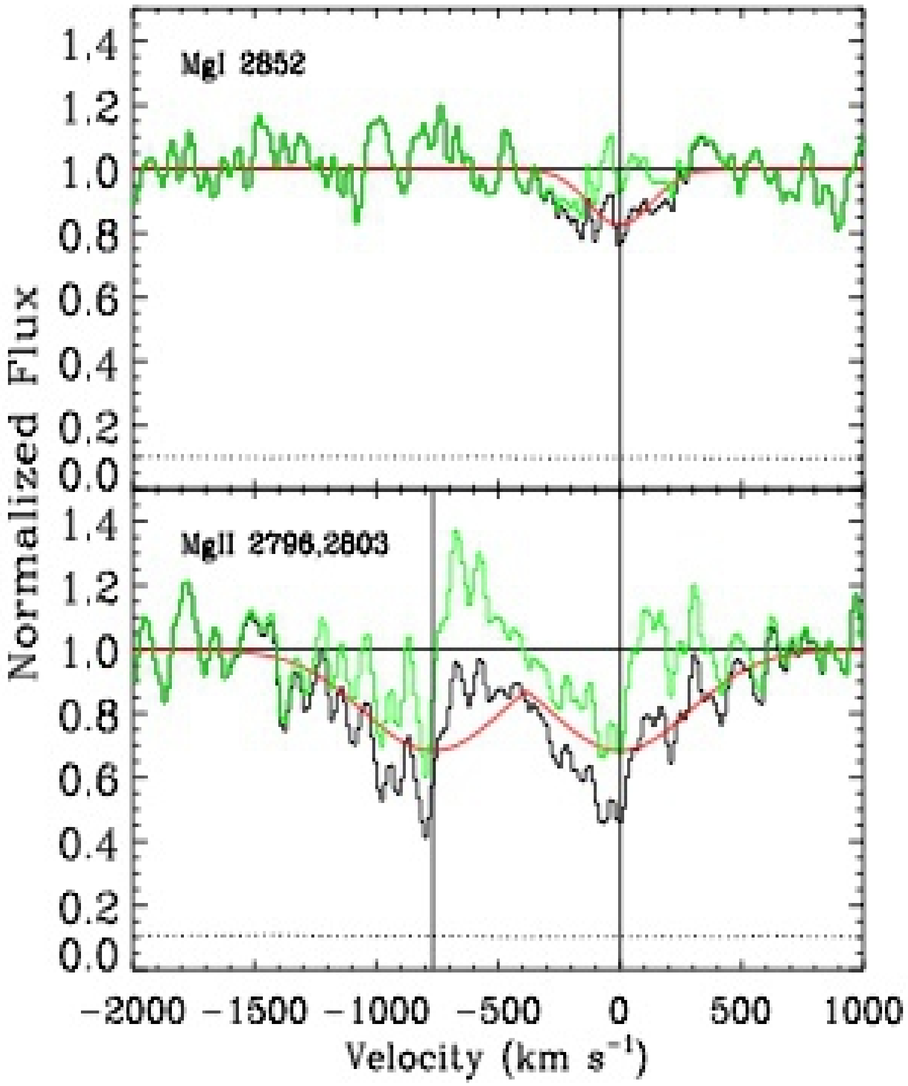

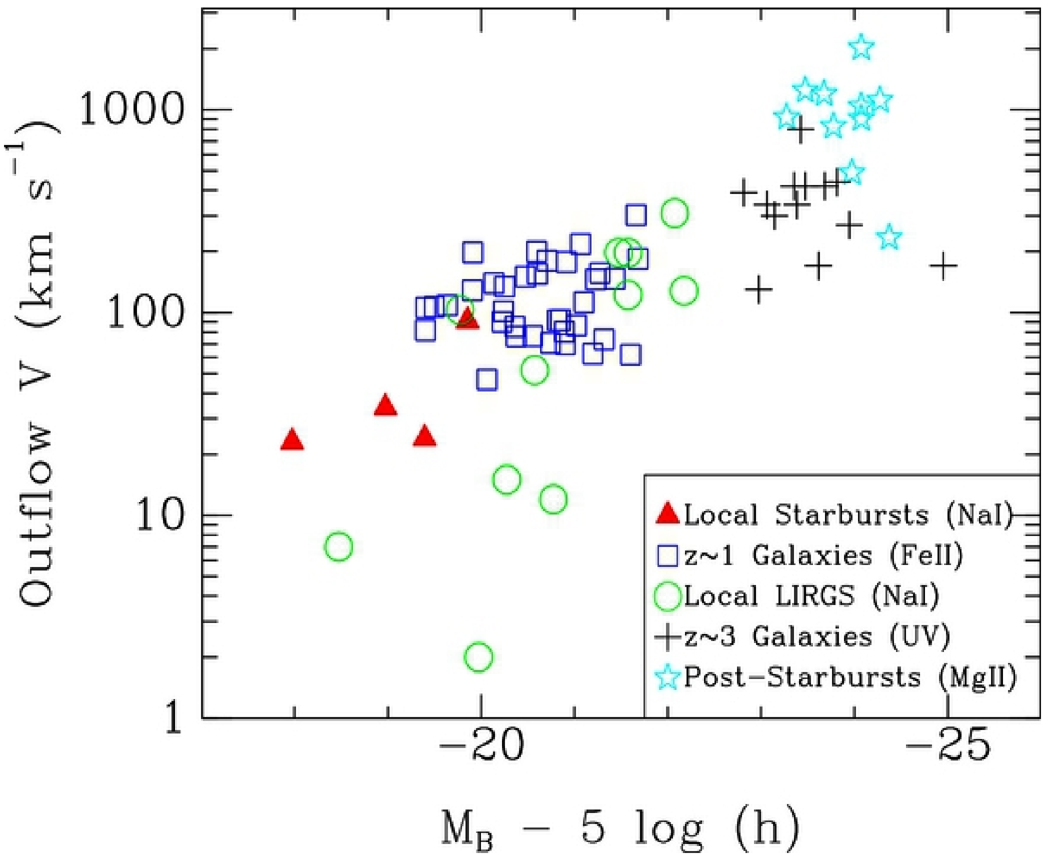

Why are high redshift galaxies more actively star-forming than nearby galaxies?
One possible scenario....

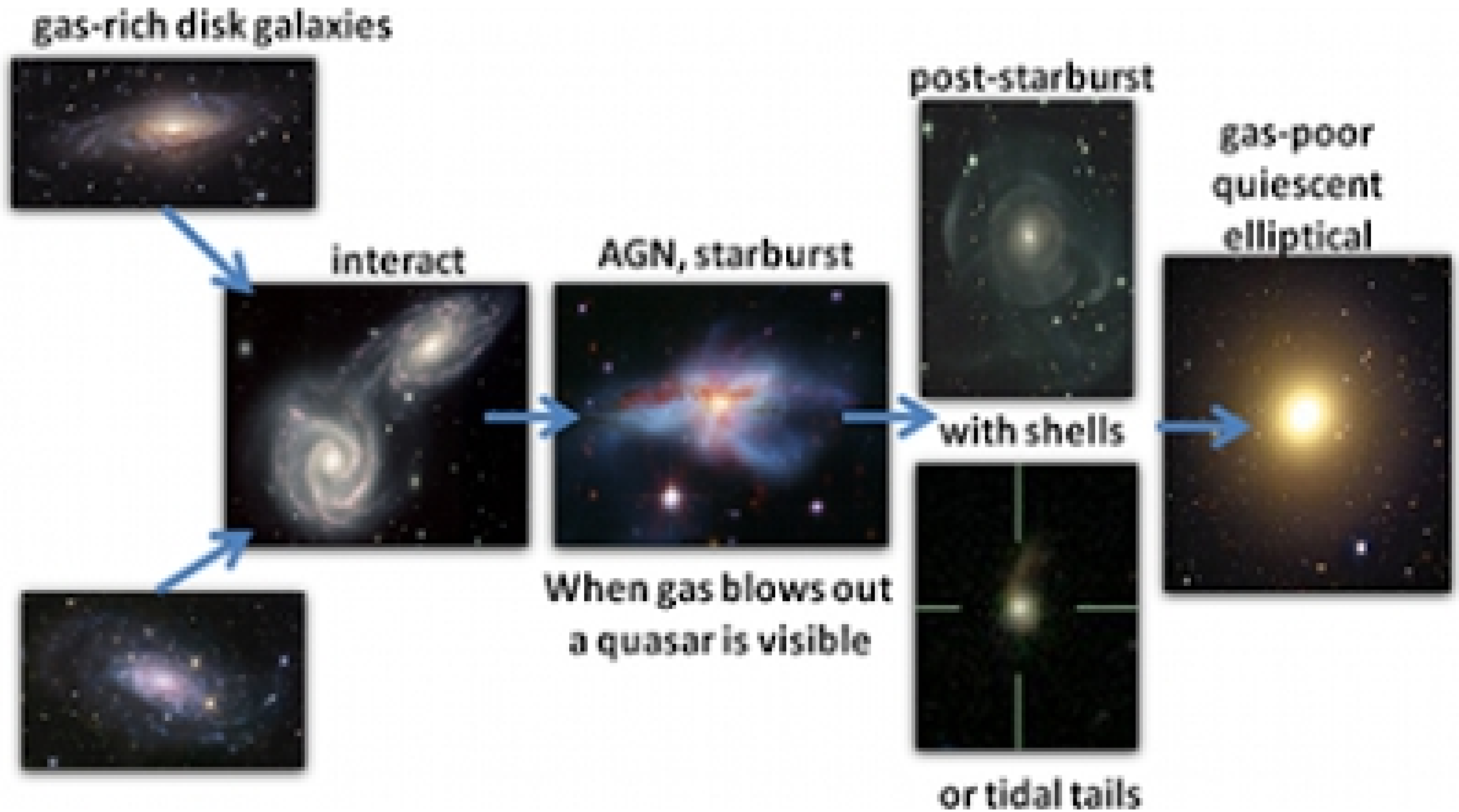

HST images allow empirical estimates of the evolution of galaxy merger rates with redshift.

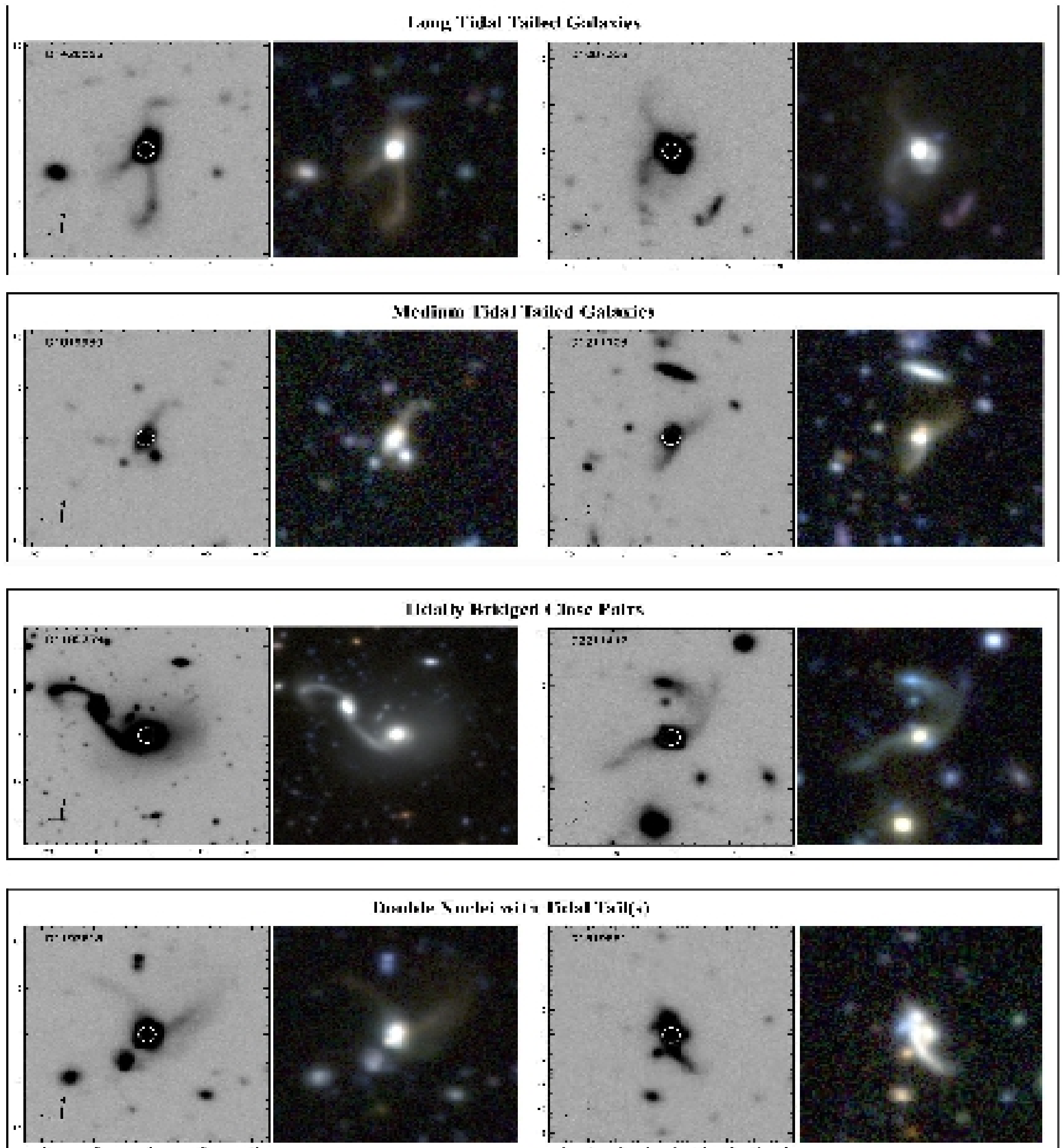

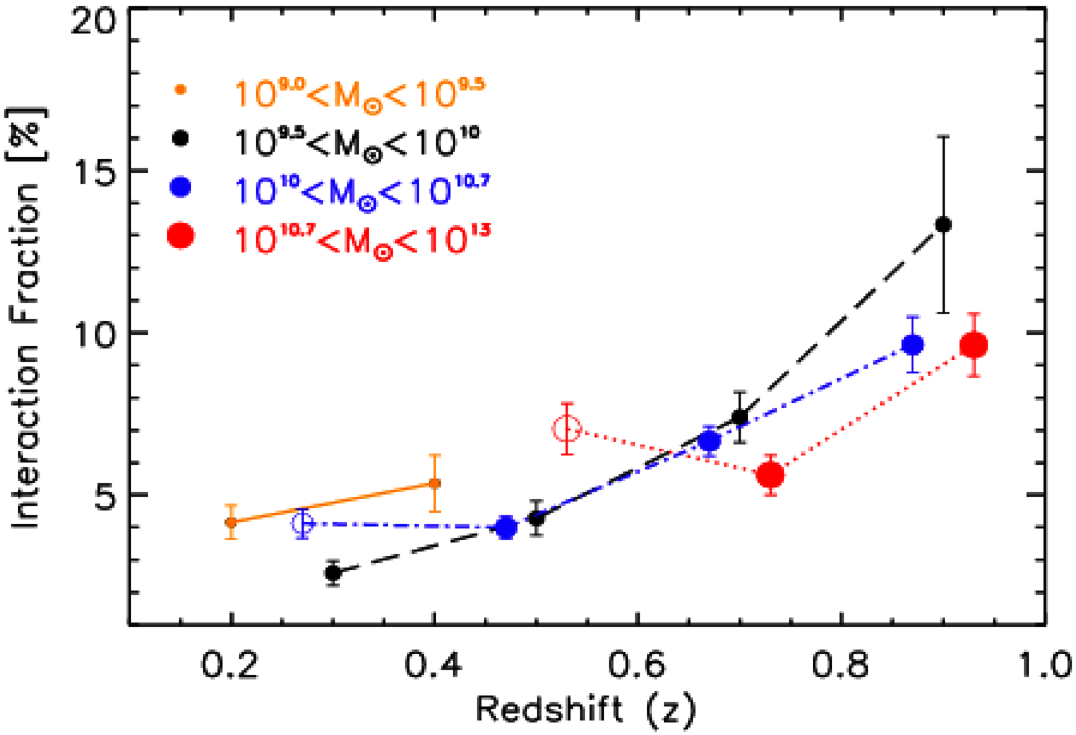

Fraction of galaxies that are visibly interacting.

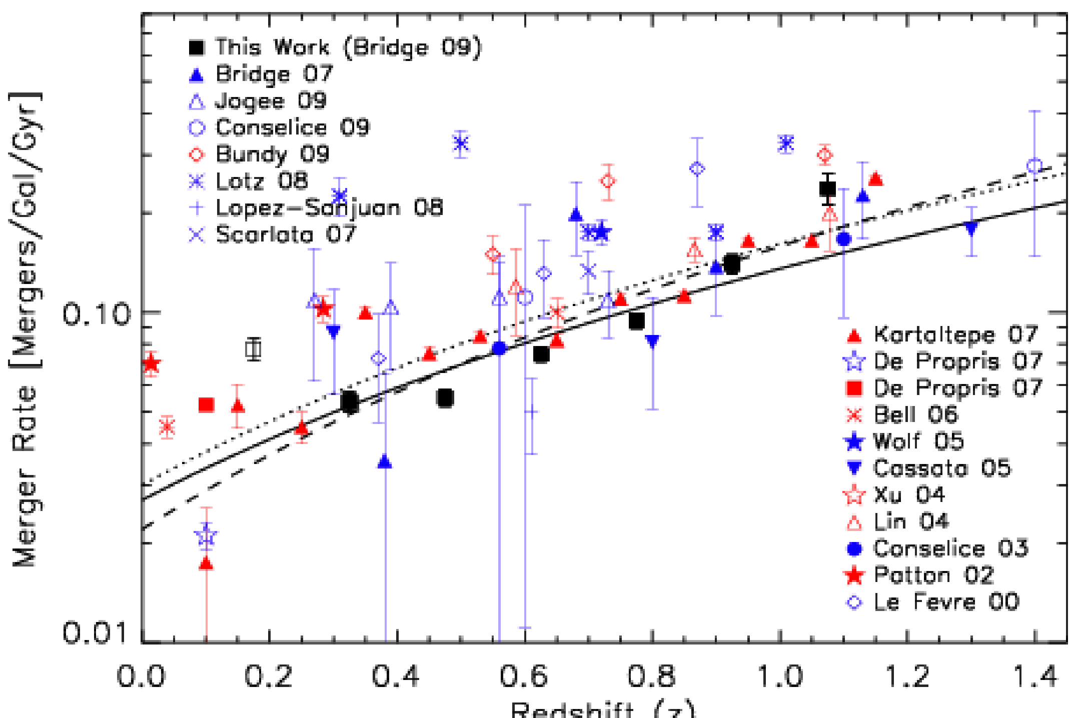

An estimate of the time interval when visible signs of the interaction are present is required to transform to merger rate.

Evolution is very mild.

Nevertheless it is clear from observations that the galaxy population has evolved significantly in size/density.

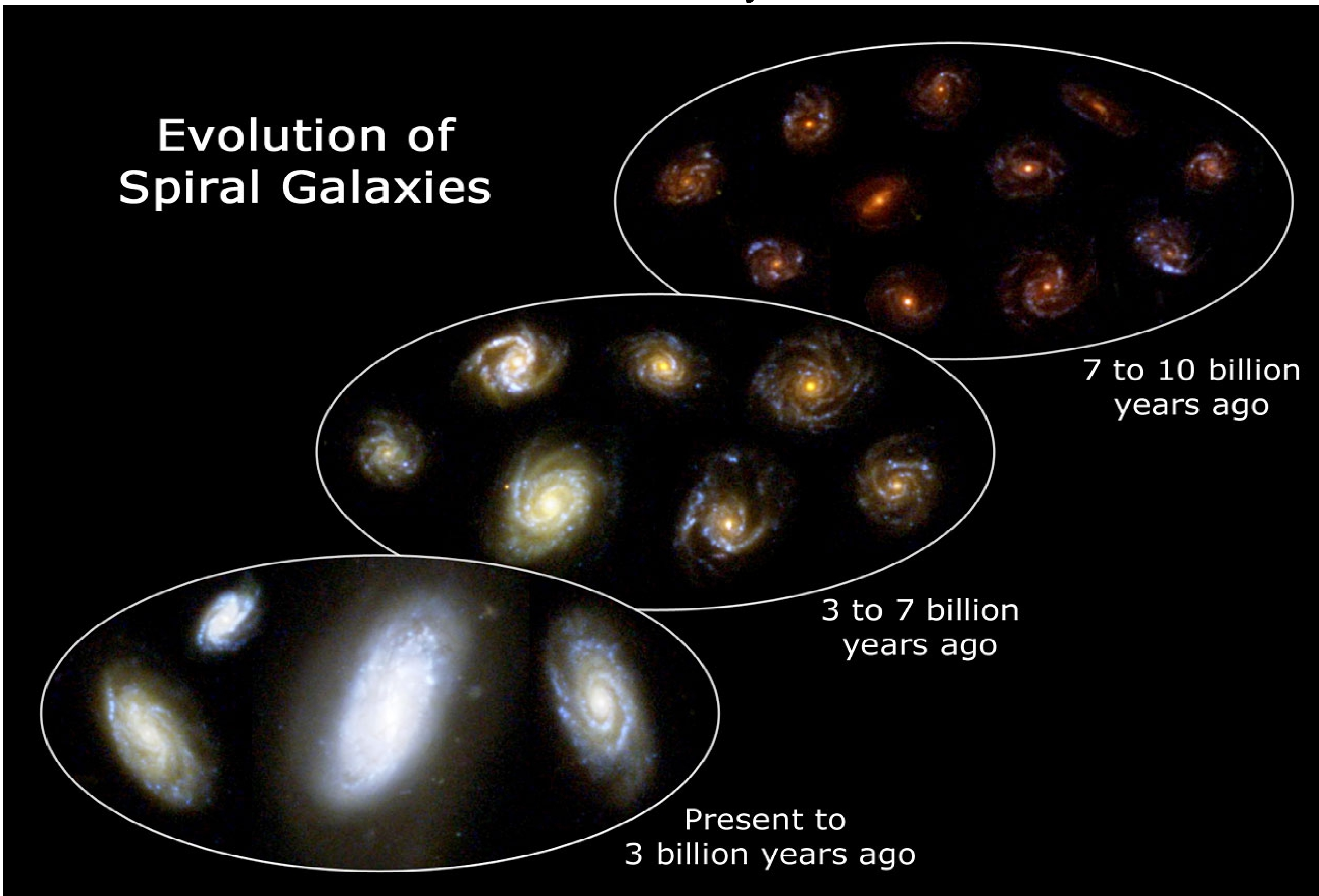

At fixed stellar mass, both early and late-type galaxies are smaller (more compact) at higher redshifts. **Poorly understood:** if not detectable mergers, what is the main mechanism controlling their growth?

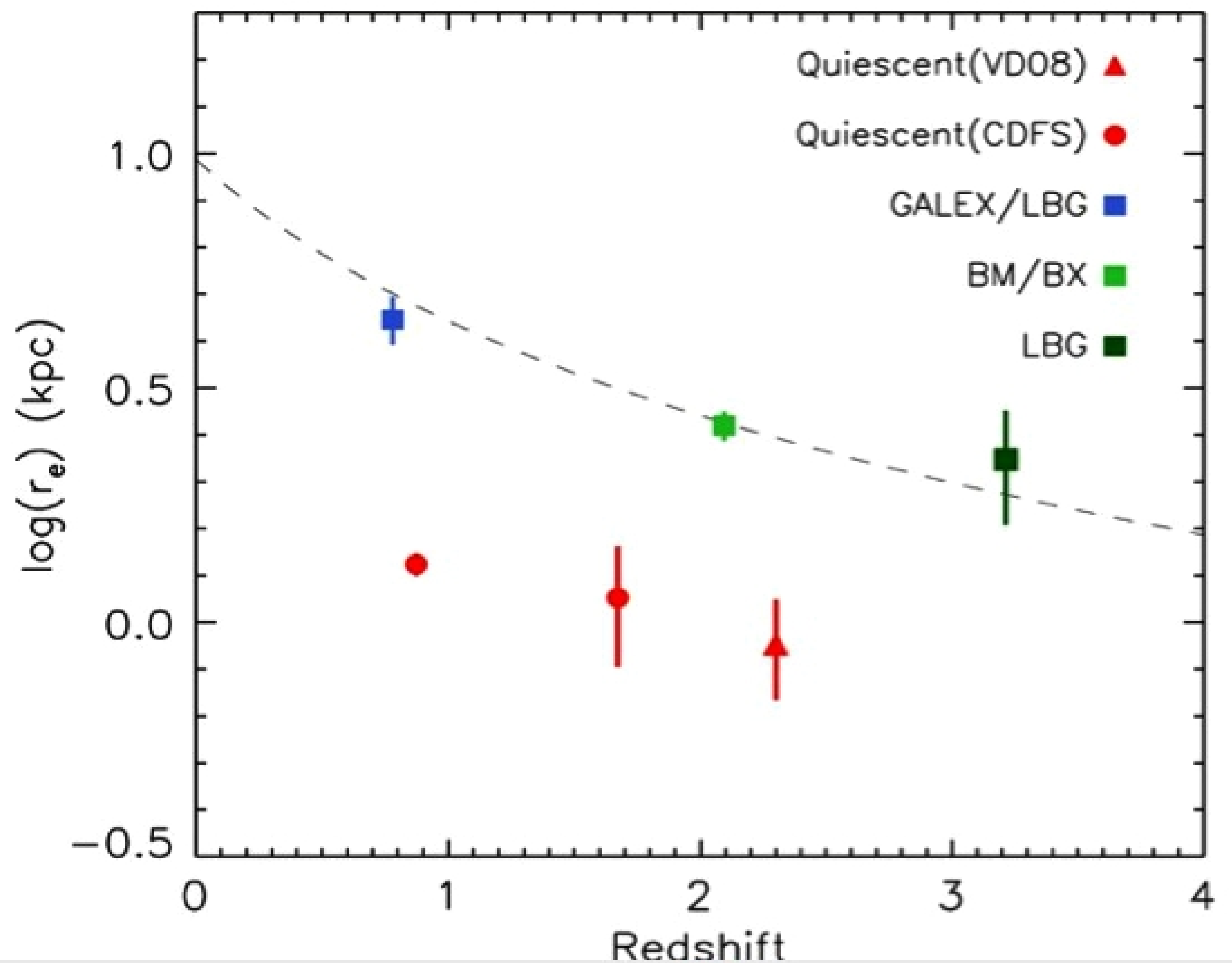

Reset

Figure 10. Median sizes of UV-bright galaxies (squares) as a function of redshifts for galaxies with stellar masses $10^{10} < M/M_\odot < 10^{11}$ in GOODS-N field. The red filled circles are quiescent galaxies from CDF-S study with similar mass range and the red triangle is the quiescent sample from van Dokkum et al. (2008b) with median stellar masses of 1.7×10^{11} $M_\odot$. The dashed line shows the best-fitting size evolution to the UV-bright galaxies ($r_e \propto (1 + z)^{-1.11\pm0.13}$). The plot indicates that the UV-selected

What about environmental effects? Galaxies in high density regions of the Universe are passive, those in low density environments are actively forming stars. As the Universe evolves, the number density of massive groups and clusters increases.

Is this sufficient to explain the observed evolution in star-forming activity?

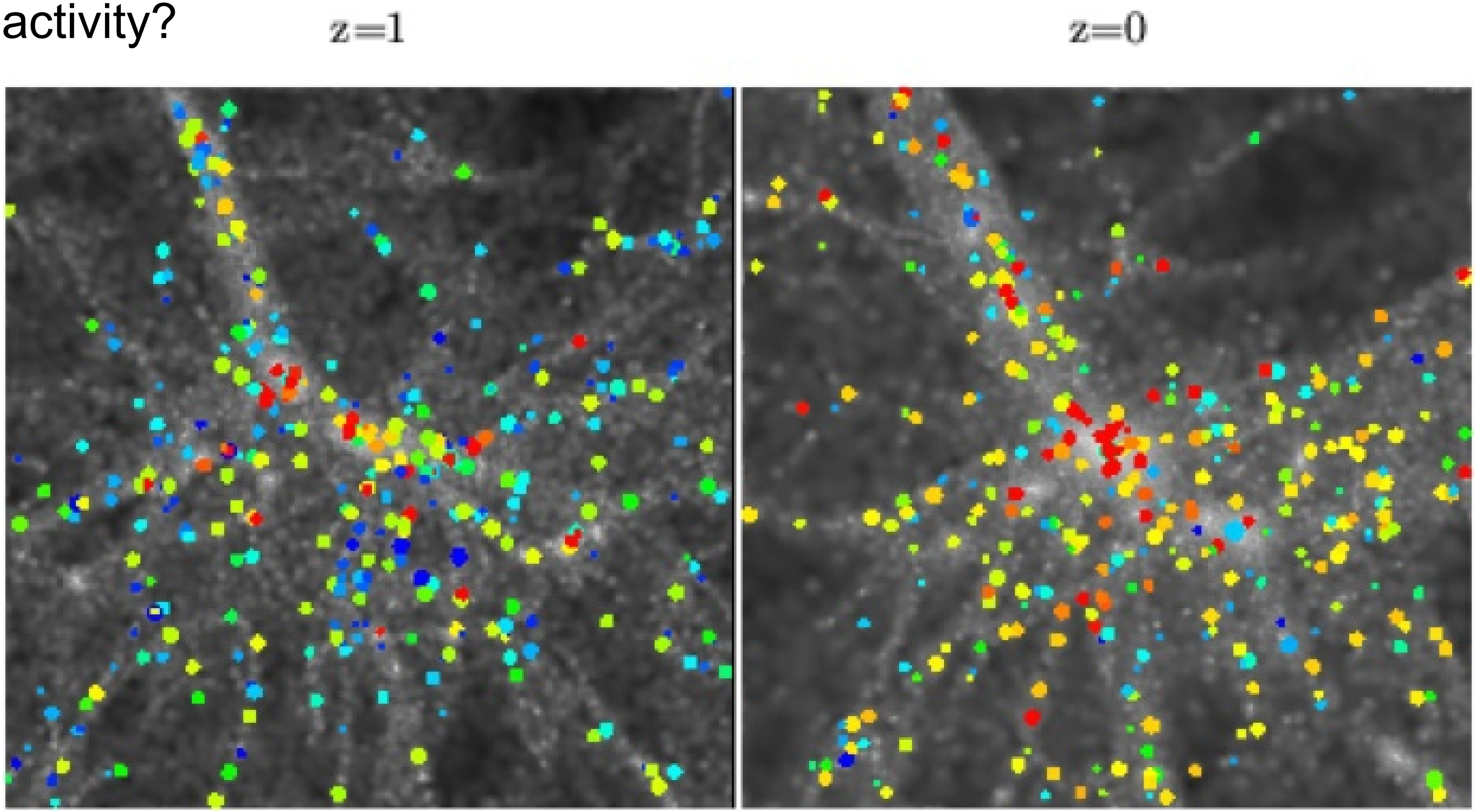

The answer from **observations** is a clear NO. The strongest evolution in star-forming activity is seen for galaxies in low density environments.

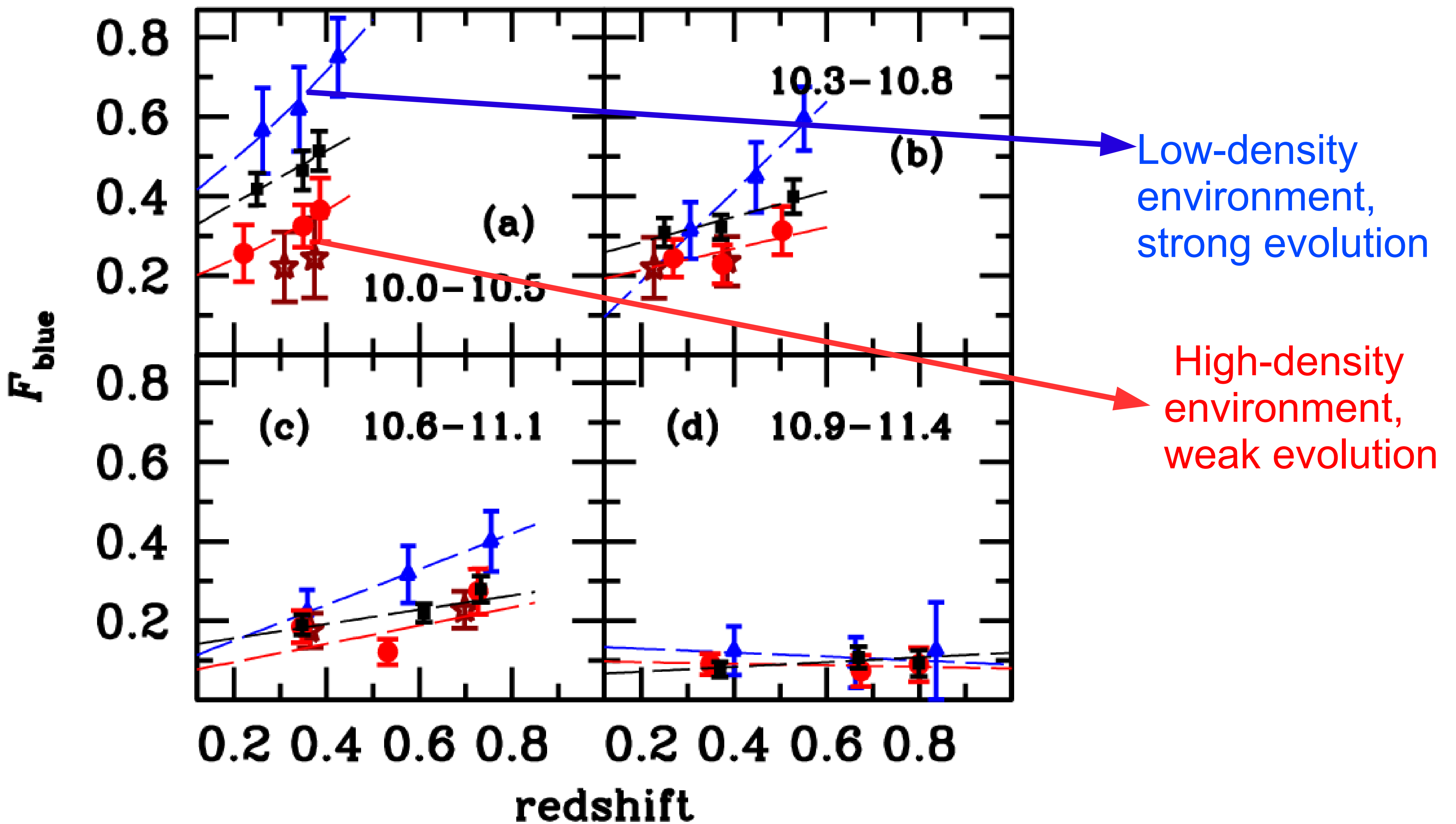

Poorly understood: what role do black holes/active galactic nuclei play in regulating galaxy growth?

Number density of galaxies with black holes that are actively accreting mass also exhibits a rise and fall, with a peak at redshifts 2-3, prompting speculation that similar behaviour of the cosmic star formation rate density may be linked.

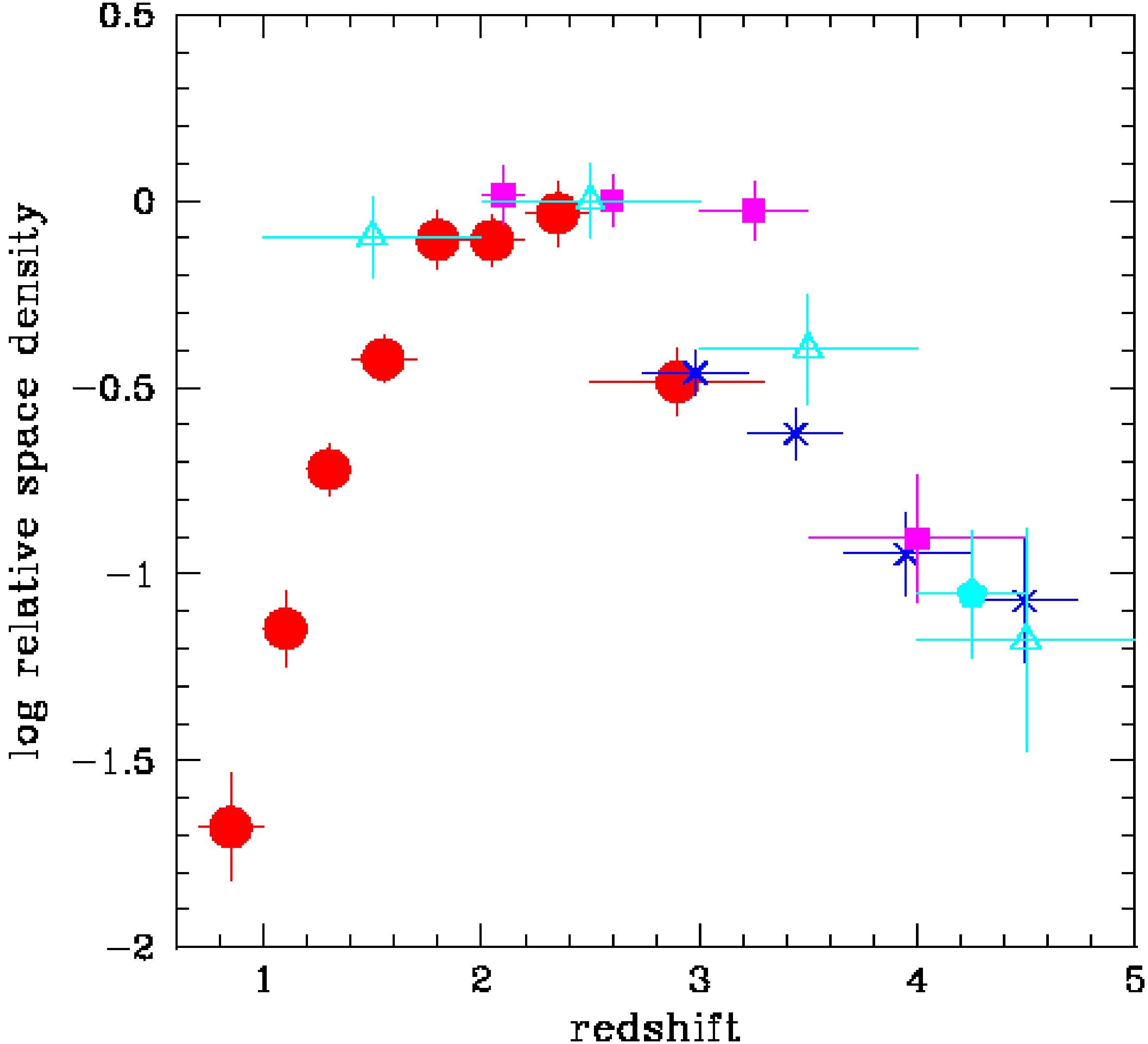

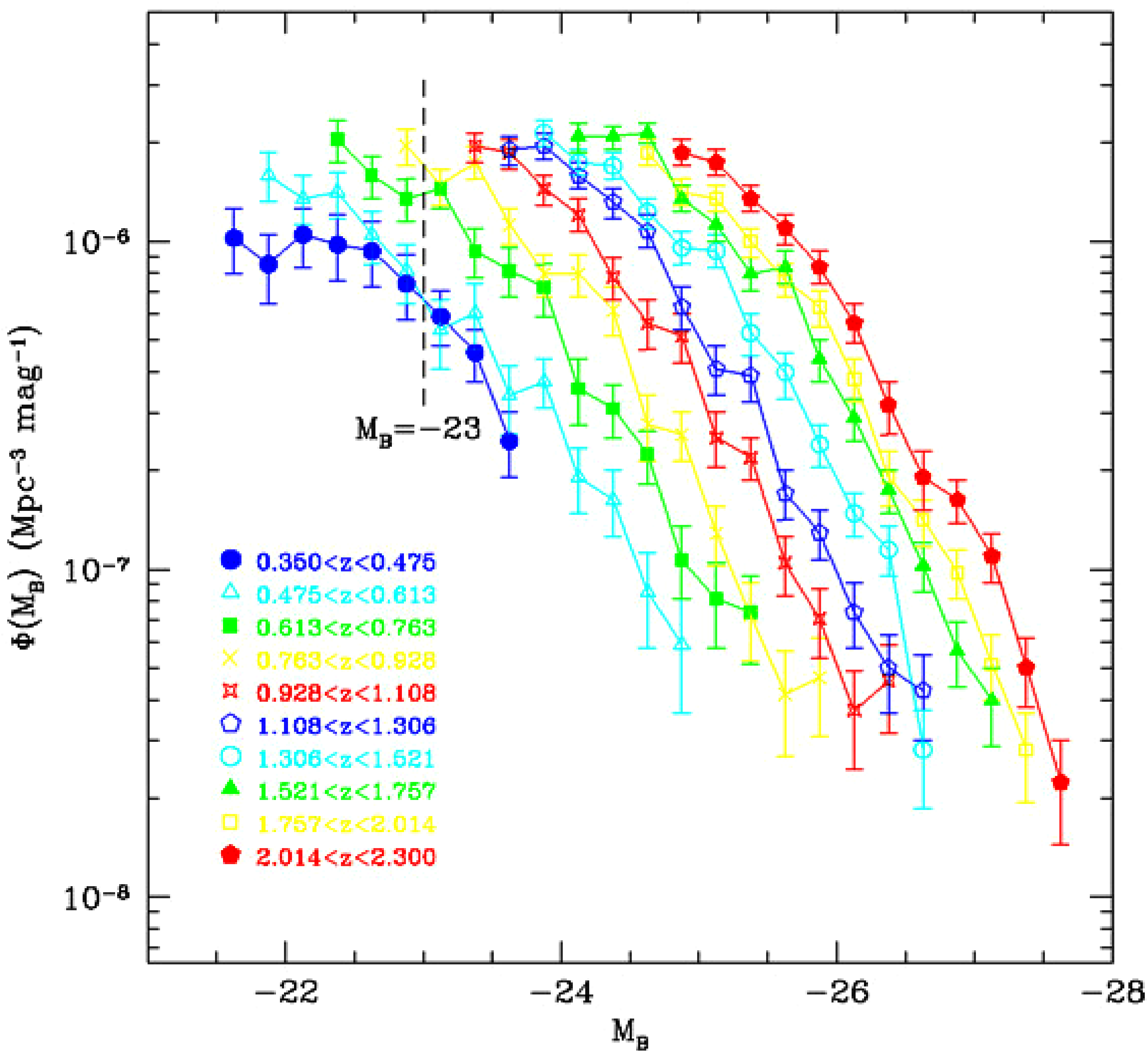

Φ(M_B) (Mpc^-3 mag^-1)
M_B
M_B=−23
0.350<z<0.475
0.475<z<0.613
0.613<z<0.763
0.763<z<0.928
0.928<z<1.108
1.108<z<1.306
1.306<z<1.521
1.521<z<1.757
1.757<z<2.014
2.014<z<2.300
10^-6
10^-7
10^-8
−22
−24
−26
−28

SUMMARY OF CURRENT SITUATION

Thanks to around 15 years heavy investment of large telescope time in observing high redshift galaxies, evolution of the global properties of the galaxy population (mass, star formation rate, size) is now quite well quantified from z=3-4 to z=0.

Robust constraints on the physical mechanisms responsible for the observed evolution are still few and far between. Not enough work has been done to interpret the observations in the framework of galaxy formation models in the standard LCDM cosmology.

(some thoughts on this to follow in my last lecture)